



OPPORTUNITIES PRESENTED BY
THE ENERGY TRANSITION

2018 **EAGE**
ANNUAL
80TH CONFERENCE + EXHIBITION
COPENHAGEN | DENMARK



11-14 JUNE 2018
WWW.EAGEANNUAL2018.ORG



EAGE ANNUAL
80TH CONFERENCE + EXHIBITION
COPENHAGEN | DENMARK

Compressed-sensing based land acquisition design

Felix J. Herrmann

Compressed-sensing based land acquisition design

Rajiv Kumar, Shashin Sharan, Nick Moldoveanu, and Felix J. Herrmann



SLIM 
Georgia Institute of Technology

Howe, D., Foster, M., Allen, T., Taylor, B. and Jack, I. [2008] Independent simultaneous sweeping -a method to increase the productivity of land seismic crews. 2826–2830.

Lin, T.T. and Herrmann, F.J. [2009] Designing simultaneous acquisitions with compressive sensing. EAGE Annual Conference Proceedings, EAGE, EAGE.

Oristaglio, M. [2012] SEAM Phase II—Land Seismic Challenges. The Leading Edge, 31(3), 264–266.

Mosher, C., Li, C., Williams, L., Carey, T., Olson, R., Malloy, J. and Ji, Y. [2017] Compressive Seismic Imaging: Land Vibroseis operations in Alaska. 127–131.

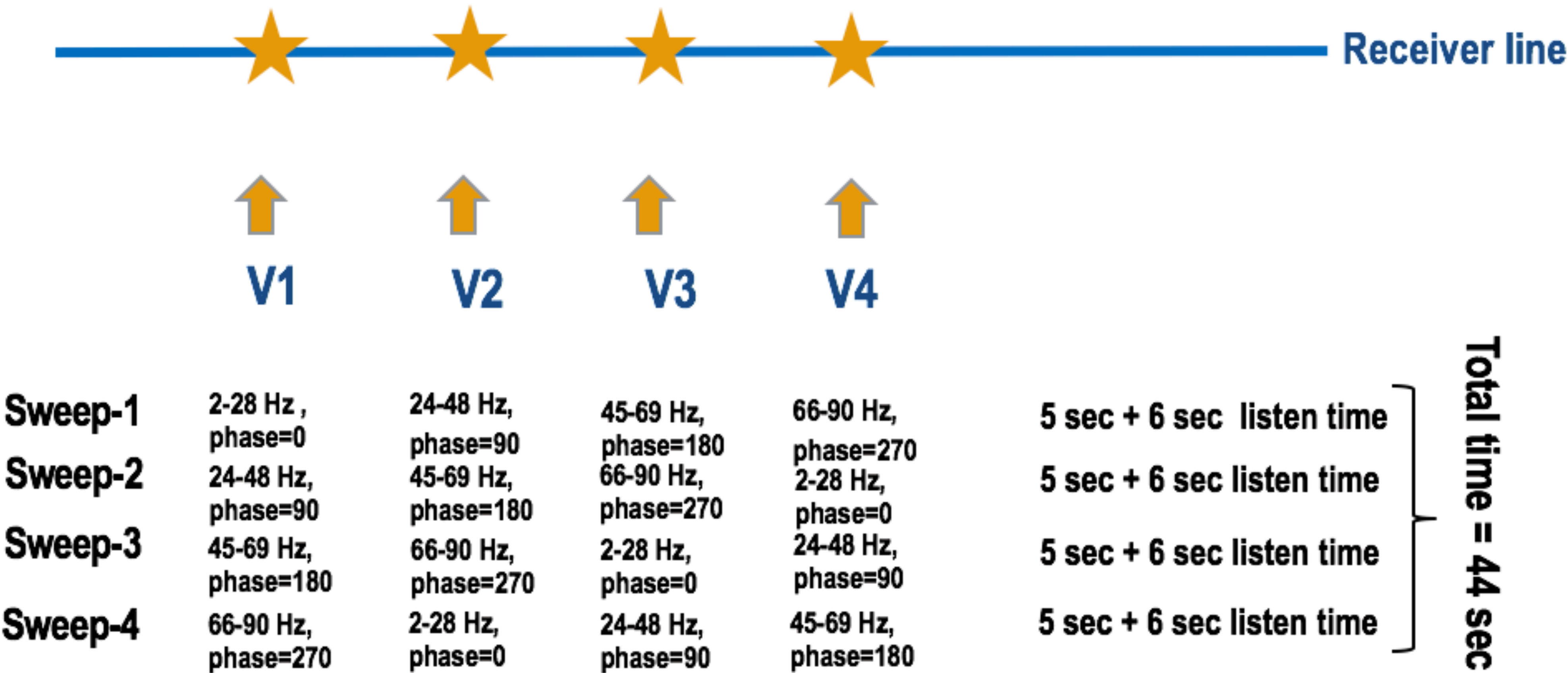
Current acquisition paradigm

Large number of single vibrators to sweep simultaneously

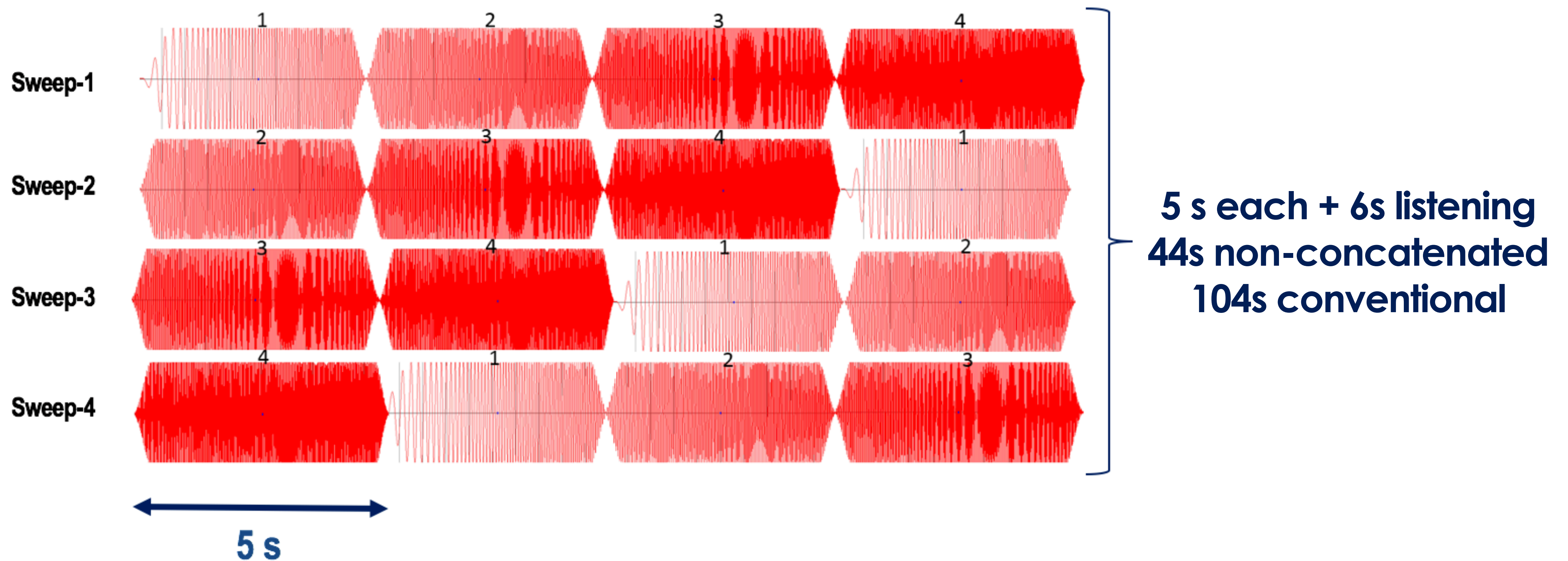
Perform source separation to recover individual shots

Cannot be used in the areas with obstruction or permit limitations

Phase- and Frequency- encoding



Phase- and Frequency- encoding



Can we further reduce the acquisition time?

Motivation

Lower the acquisition cost using simultaneous encoded sweeps

Reduce the sweeping time

Coarsely sampled data w/ insights from Compressive Sensing

Compressive sensing paradigm

Sample to break structure = renders interference into incoherent noise

- ▶ randomized acquisition (e.g., time-jittered, over/under, continuous recording etc.)
- ▶ destroys sparsity/low rank

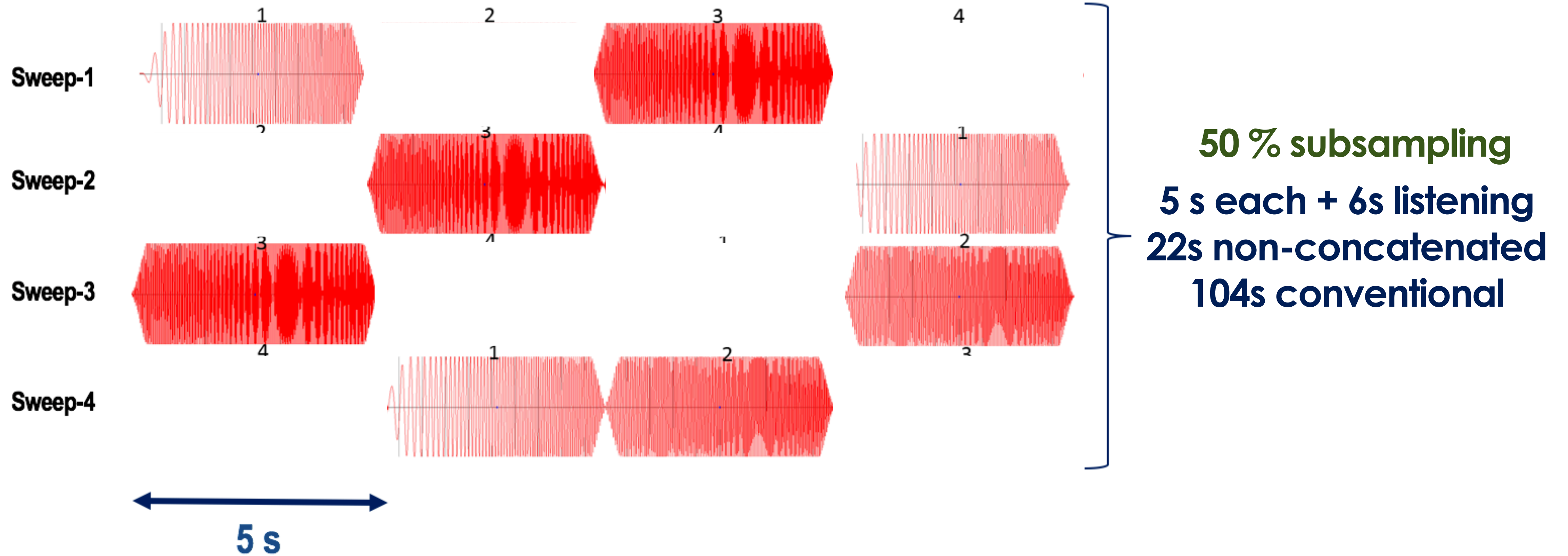
Find representations that reveal structure = separate signal from “noise”

- ▶ transform-domain sparsity (e.g., Fourier, curvelets, etc.)
- ▶ low-rank revealing matrix or tensor representations

Recover by structure promotion = obtain artifact-free densely sampled data

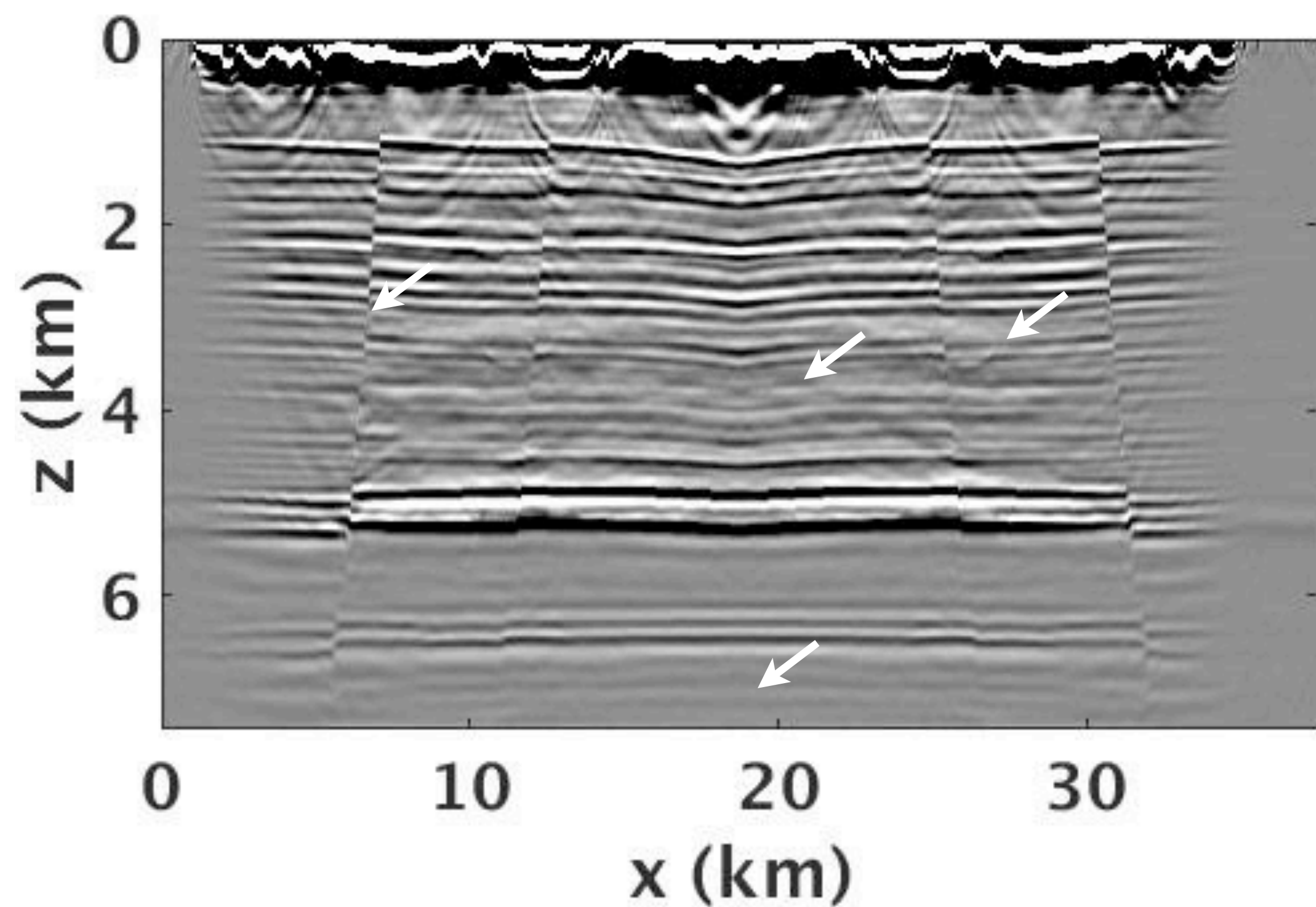
- ▶ sparsity via one-norm minimization, or
- ▶ nuclear-norm minimization

Random Phase- and Frequency- encoding

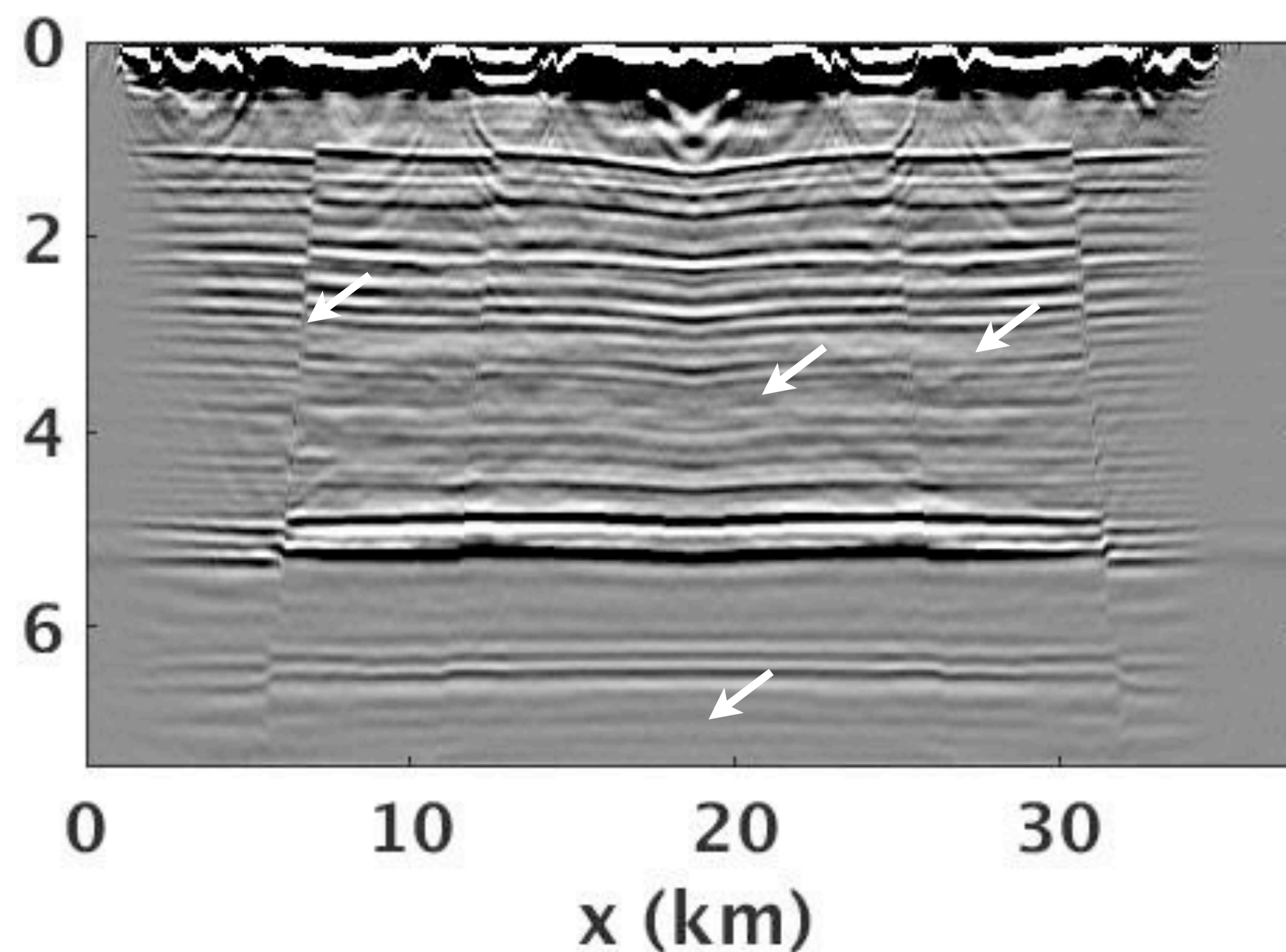


Reverse time migration

True



After deblending & Spectral Interpolation
4-5x speedup in acquisition



[Candes and Plan 2010, Oropenza and Sacchi 2011]

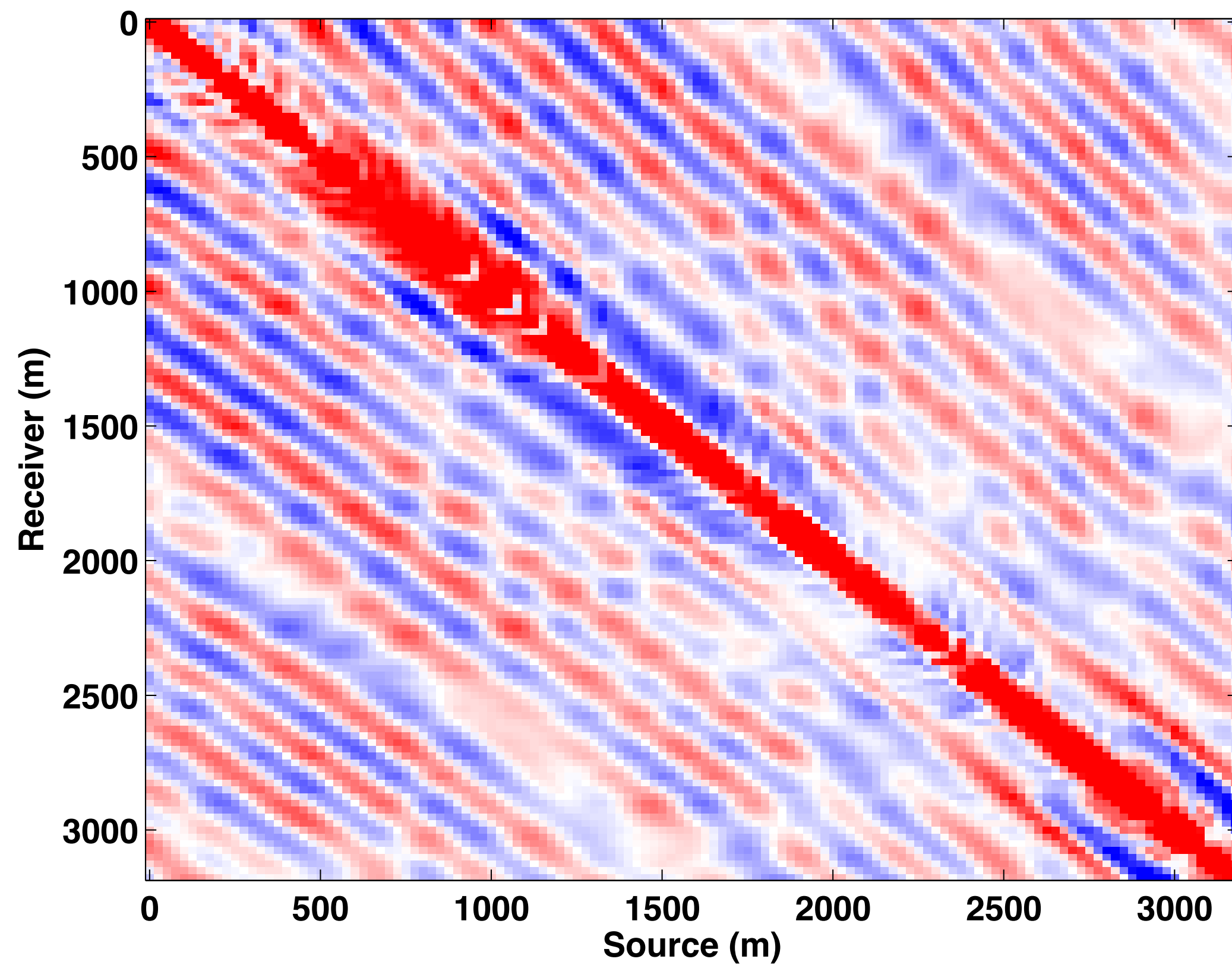
Matrix completion

- ▶ signal structure
 - *low rank/fast decay* of singular values
- ▶ sampling scheme
 - missing data *increase* rank in “transform domain”
- ▶ recovery using *rank penalization* scheme

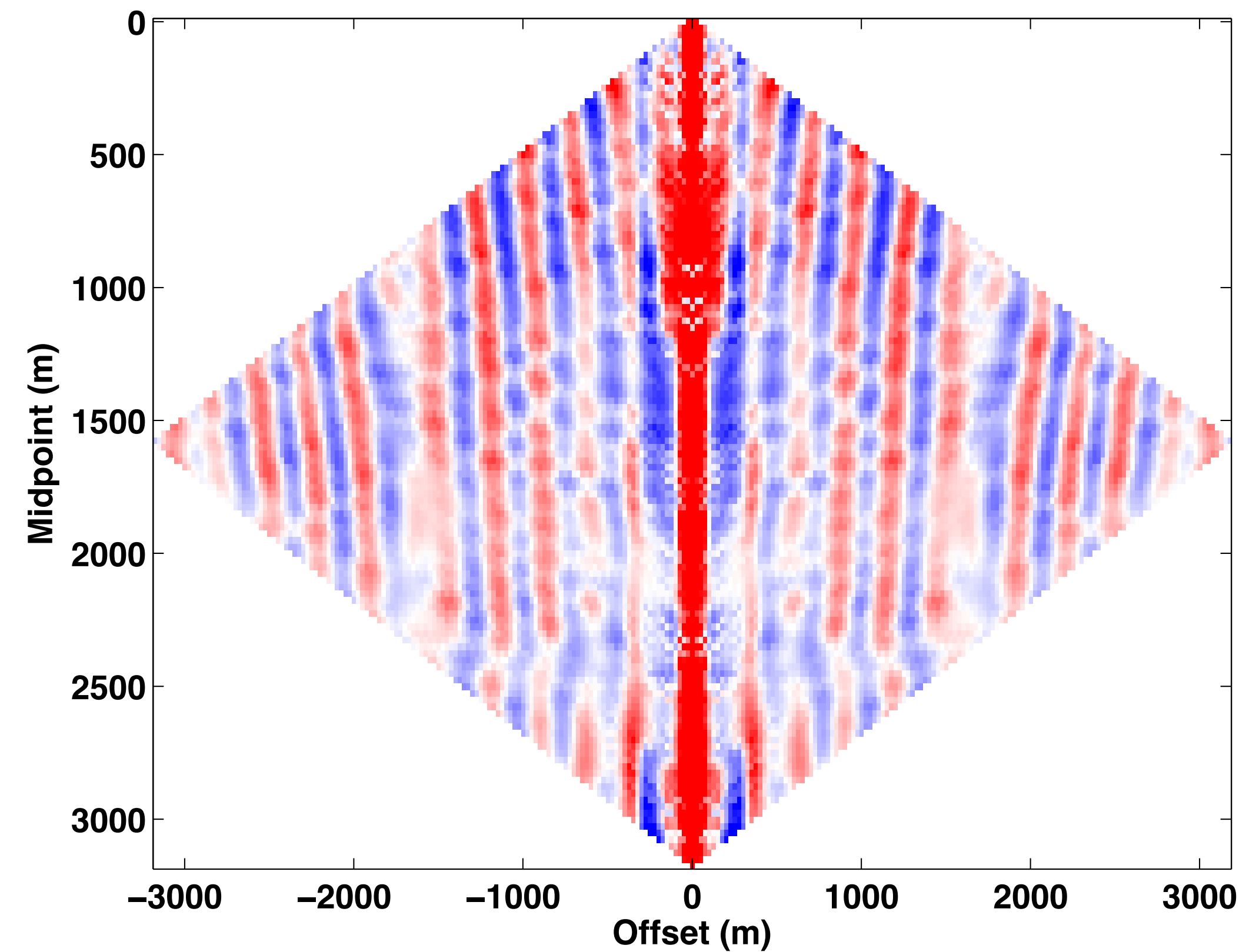
Low-rank structure

conventional 5D data, monochromatic slice

source-receiver domain

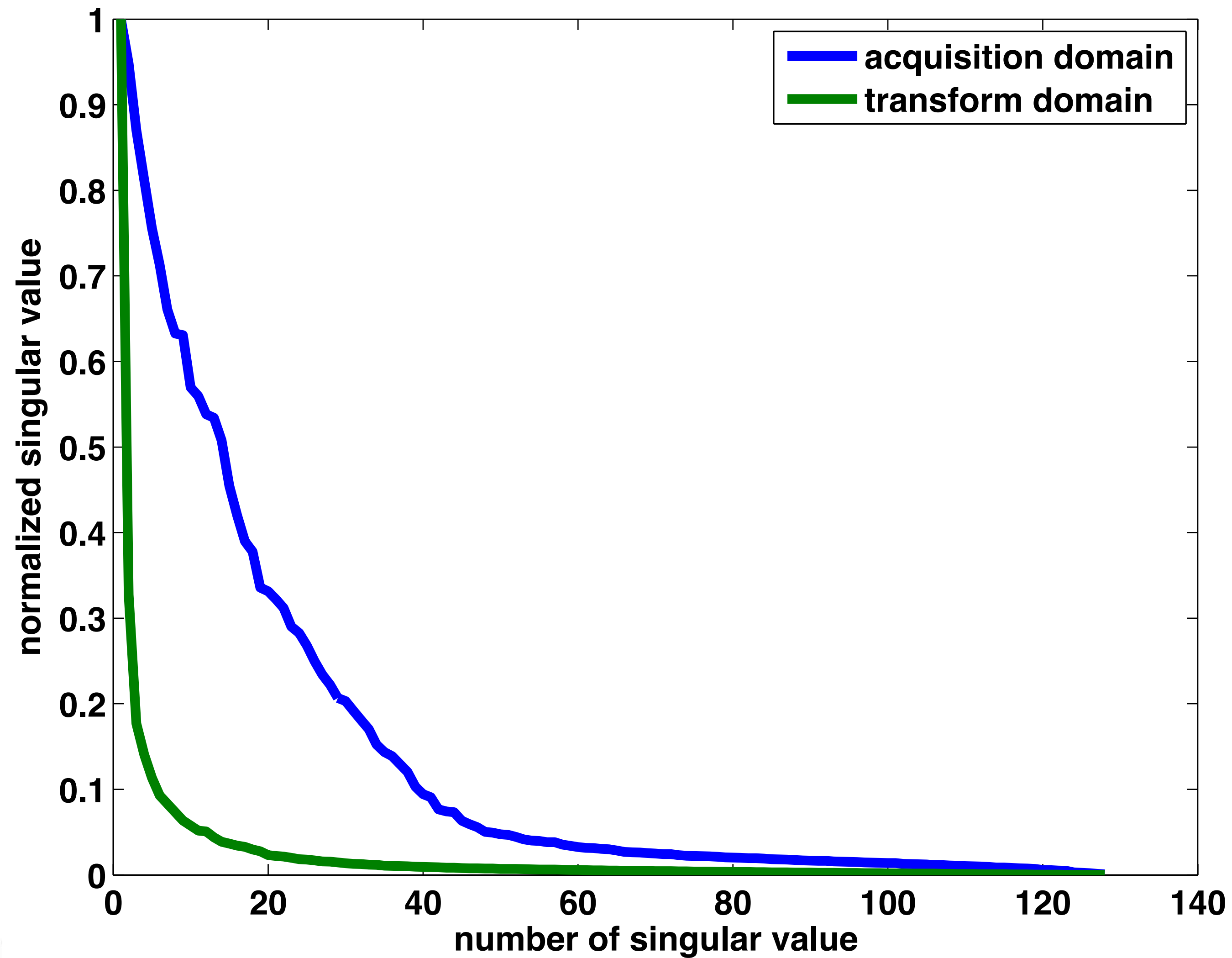


midpoint-offset domain



Low-rank structure

conventional 3D data, monochromatic slice, SVD decay



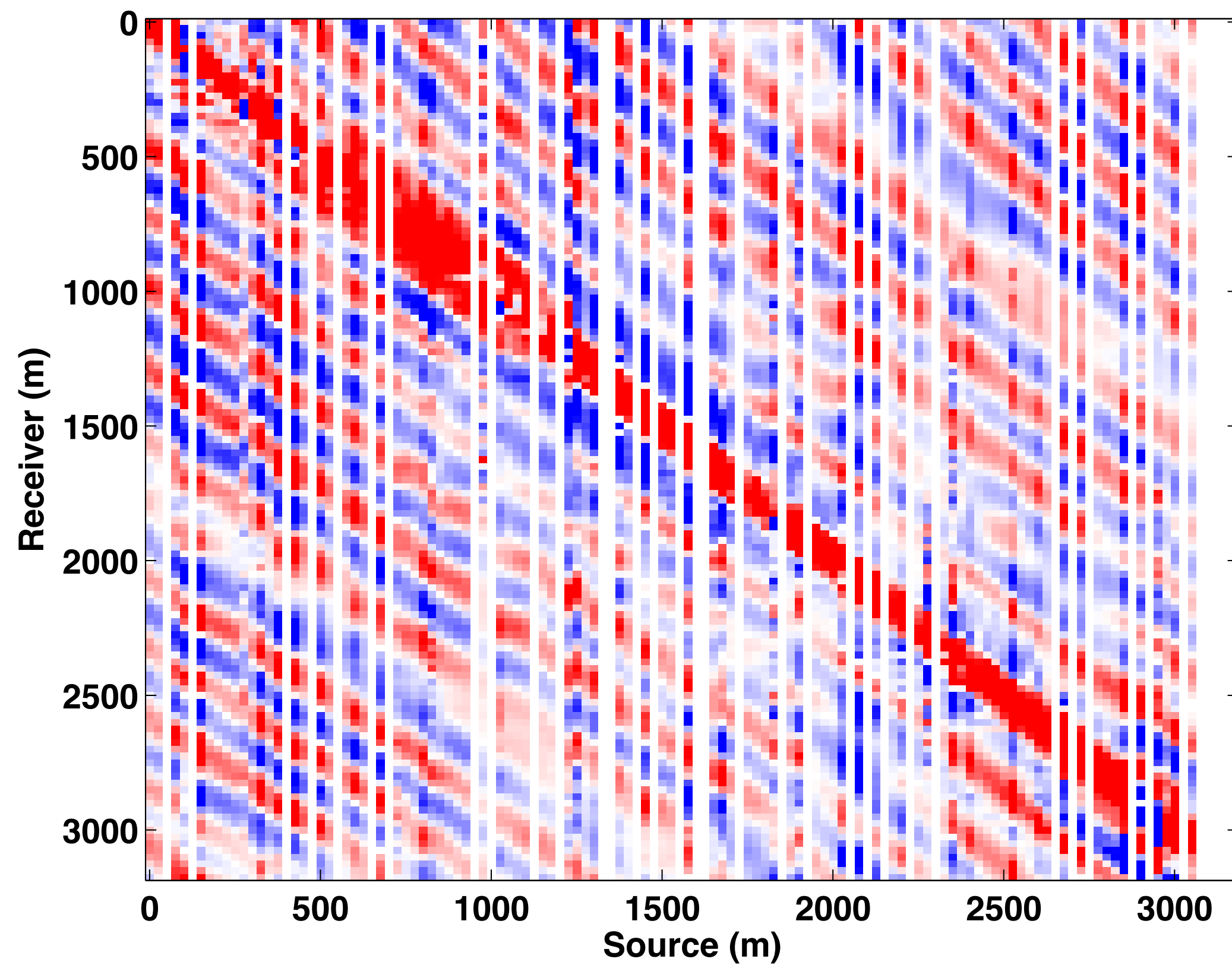
Matrix completion

- ▶ signal structure
 - *low rank/fast decay* of singular values
- ▶ sampling scheme
 - missing data *increase* rank in “transform domain”
- ▶ recovery using *rank penalization* scheme

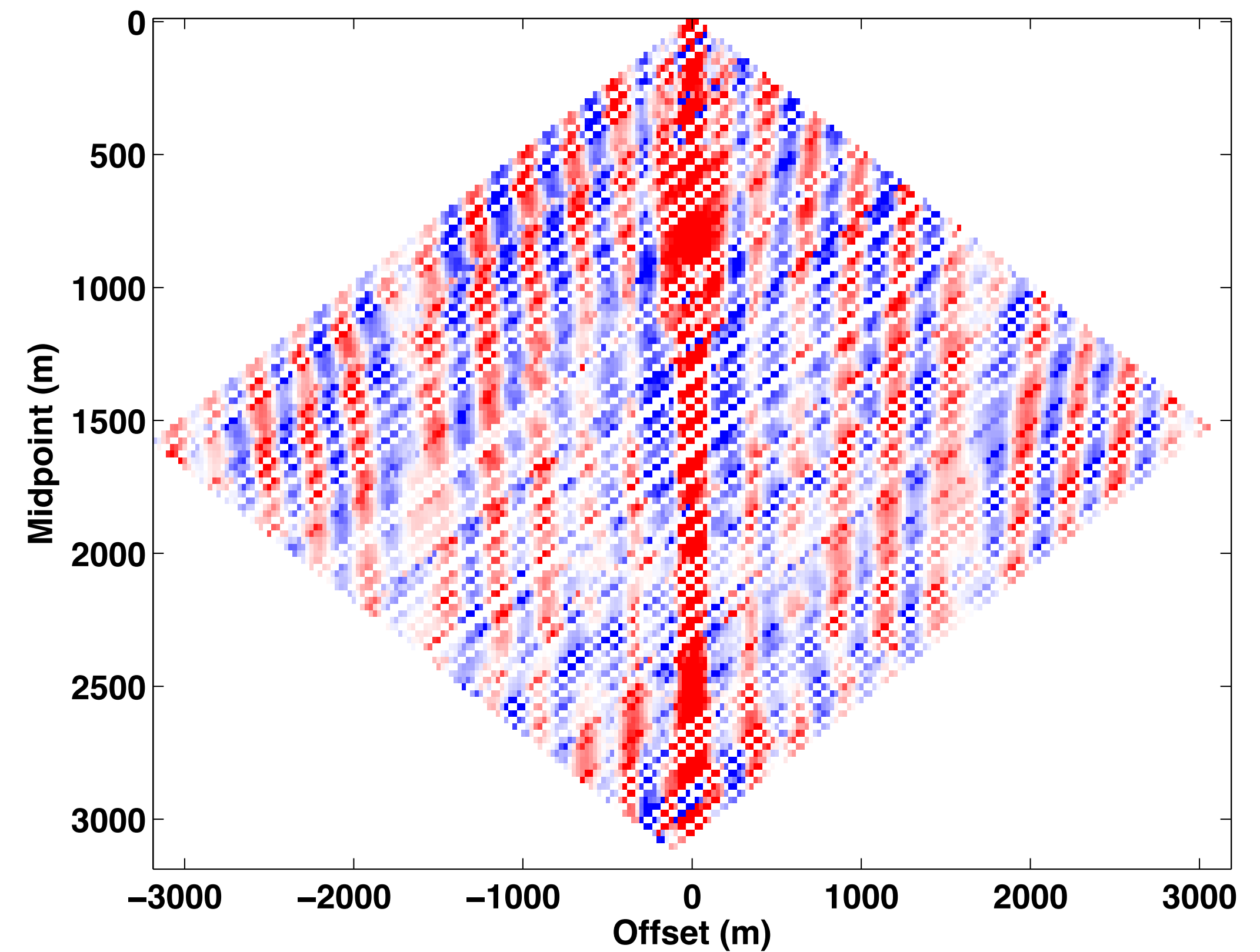
Low-rank structure

pseudo-deblended data, monochromatic slice

source-receiver domain



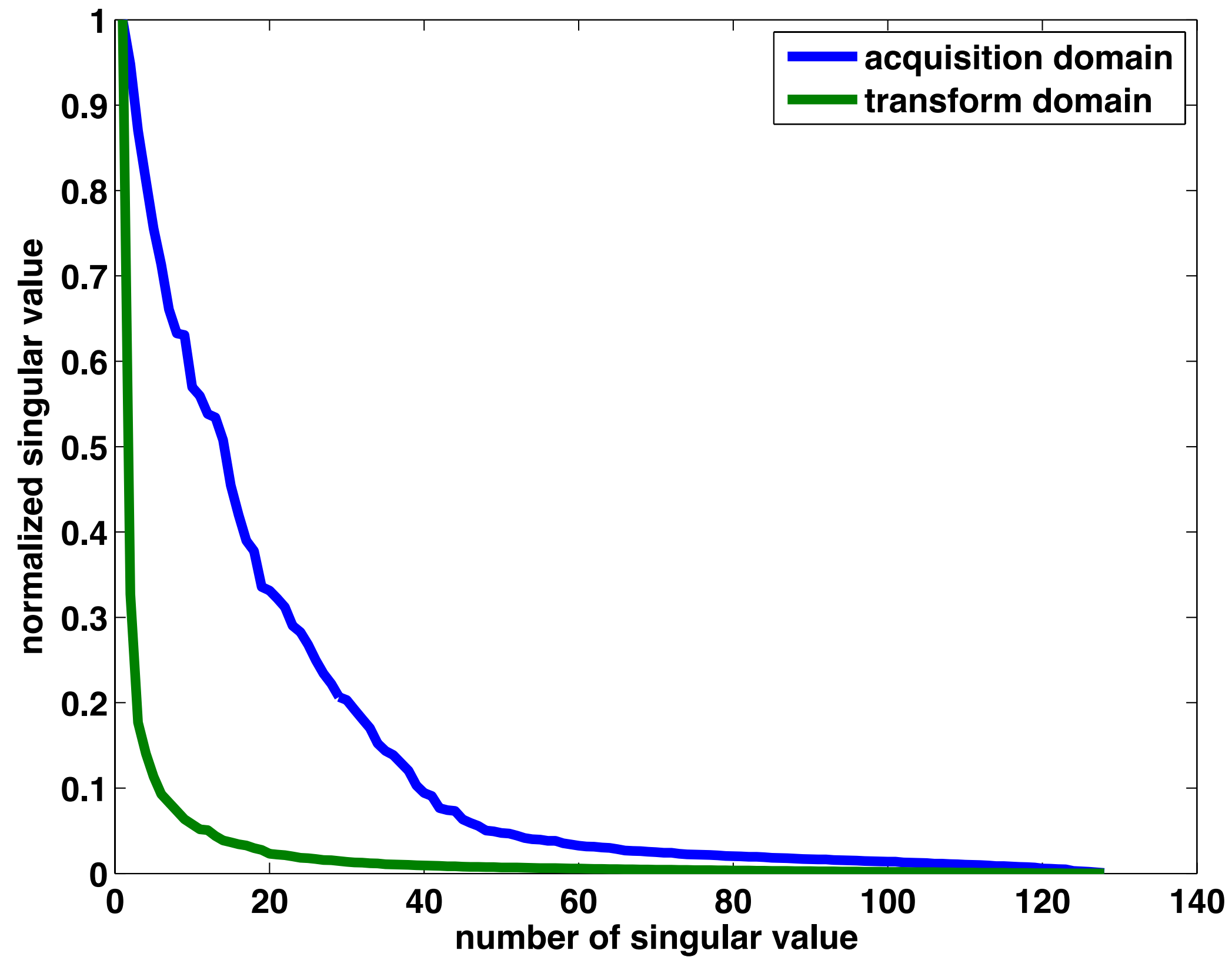
midpoint-offset domain



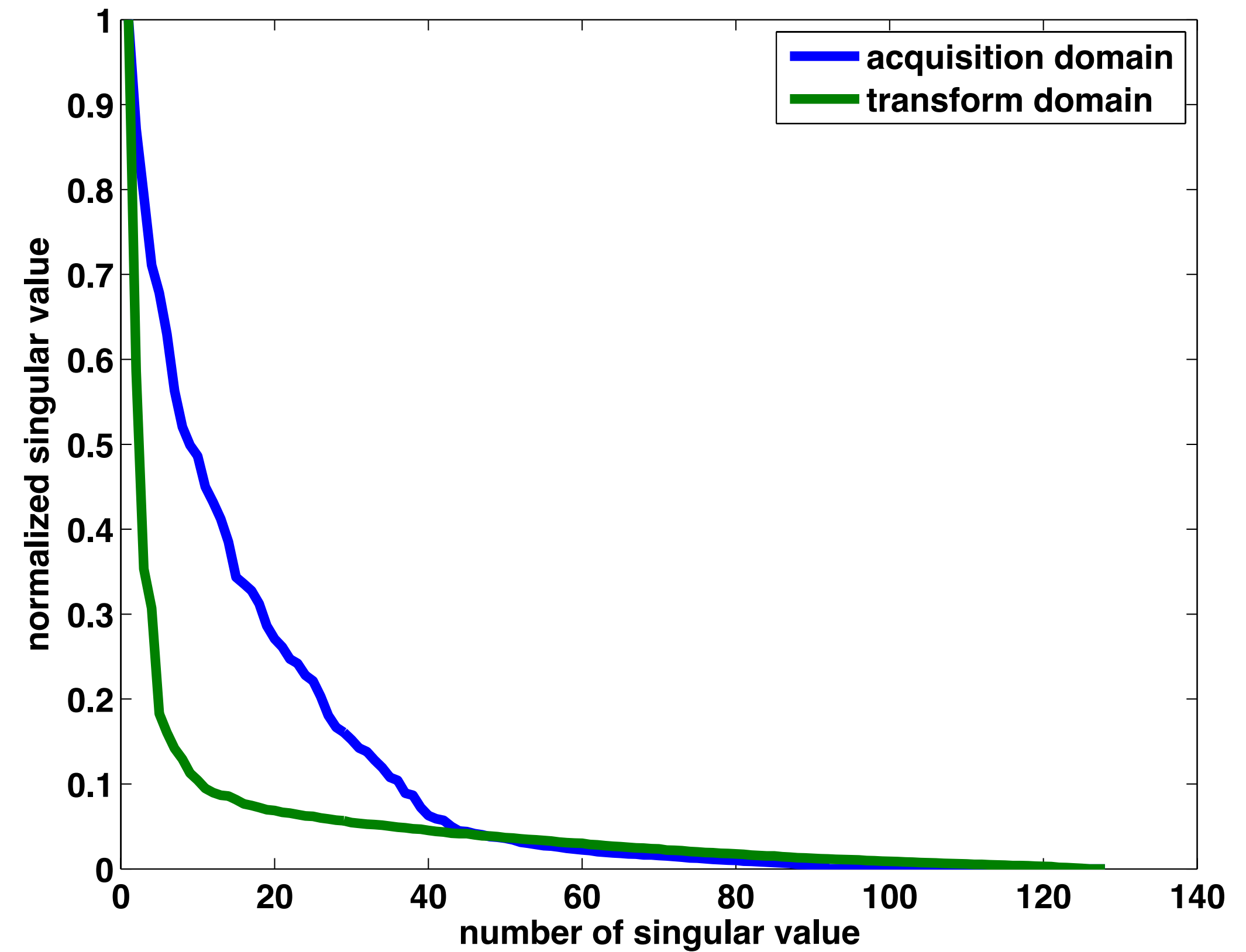
Low-rank structure

pseudo-deblended data, monochromatic slice

Fully sampled



After deblending



Matrix completion

- ▶ signal structure
 - *low rank/fast decay* of singular values
- ▶ sampling scheme
 - missing data *increase* rank in “transform domain”
- ▶ recovery using *rank penalization* scheme

Nuclear-norm minimization

[Recht et. al., 2010]

$$\min_{\mathbf{X}} \underbrace{\|\mathbf{X}\|_*}_{\text{sum of singular values of } \mathbf{X}} \quad \text{s.t.} \quad \|\mathcal{A}(\mathbf{X}) - \mathbf{b}\|_2 \leq \epsilon$$

where

$$\mathcal{A} = \mathbf{F}_t^{-1} \mathbf{R} \mathbf{B} \mathcal{S}^H$$

F Temporal-Fourier transform

R Restriction operator

S Midpoint-offset operator

B Blending and convolution operator

Nuclear-norm minimization

[Recht et. al., 2010]

$$\mathbf{B} = \begin{bmatrix} \mathbf{B}_1 & & & \\ & \ddots & & \\ & & \mathbf{B}_k & \end{bmatrix}$$

where

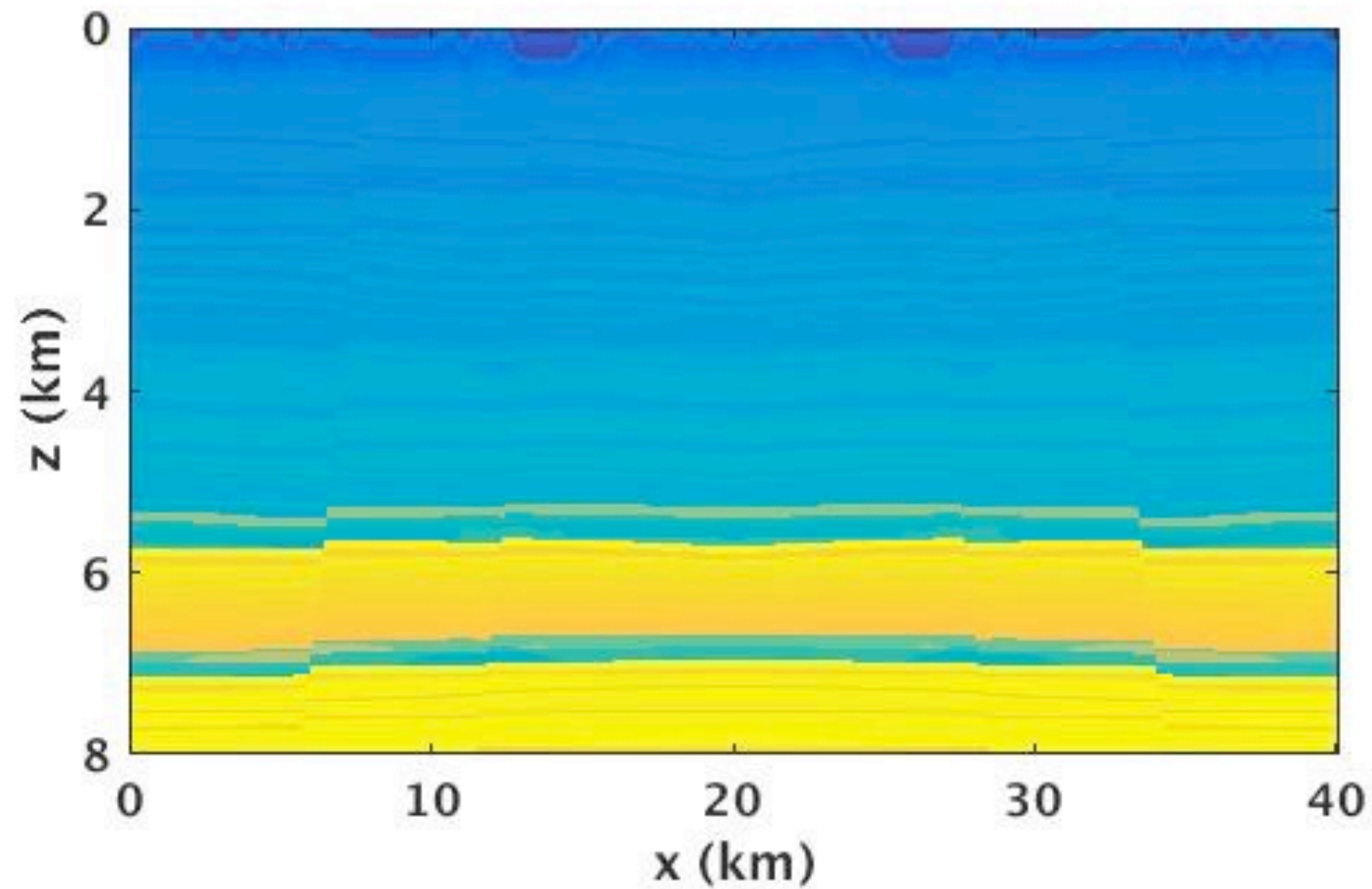
$$\mathbf{B}_i = \begin{pmatrix} \text{diag}(a_1) & \text{diag}(a_2) & \text{diag}(a_3) & \text{diag}(a_4) \\ \text{diag}(a_2) & \text{diag}(a_3) & \text{diag}(a_4) & \text{diag}(a_1) \\ \text{diag}(a_3) & \text{diag}(a_4) & \text{diag}(a_1) & \text{diag}(a_2) \\ \text{diag}(a_4) & \text{diag}(a_1) & \text{diag}(a_2) & \text{diag}(a_3) \end{pmatrix}$$

a_1, a_2, a_3, a_4 Four sweep segments and $k = \frac{N_s}{n}$

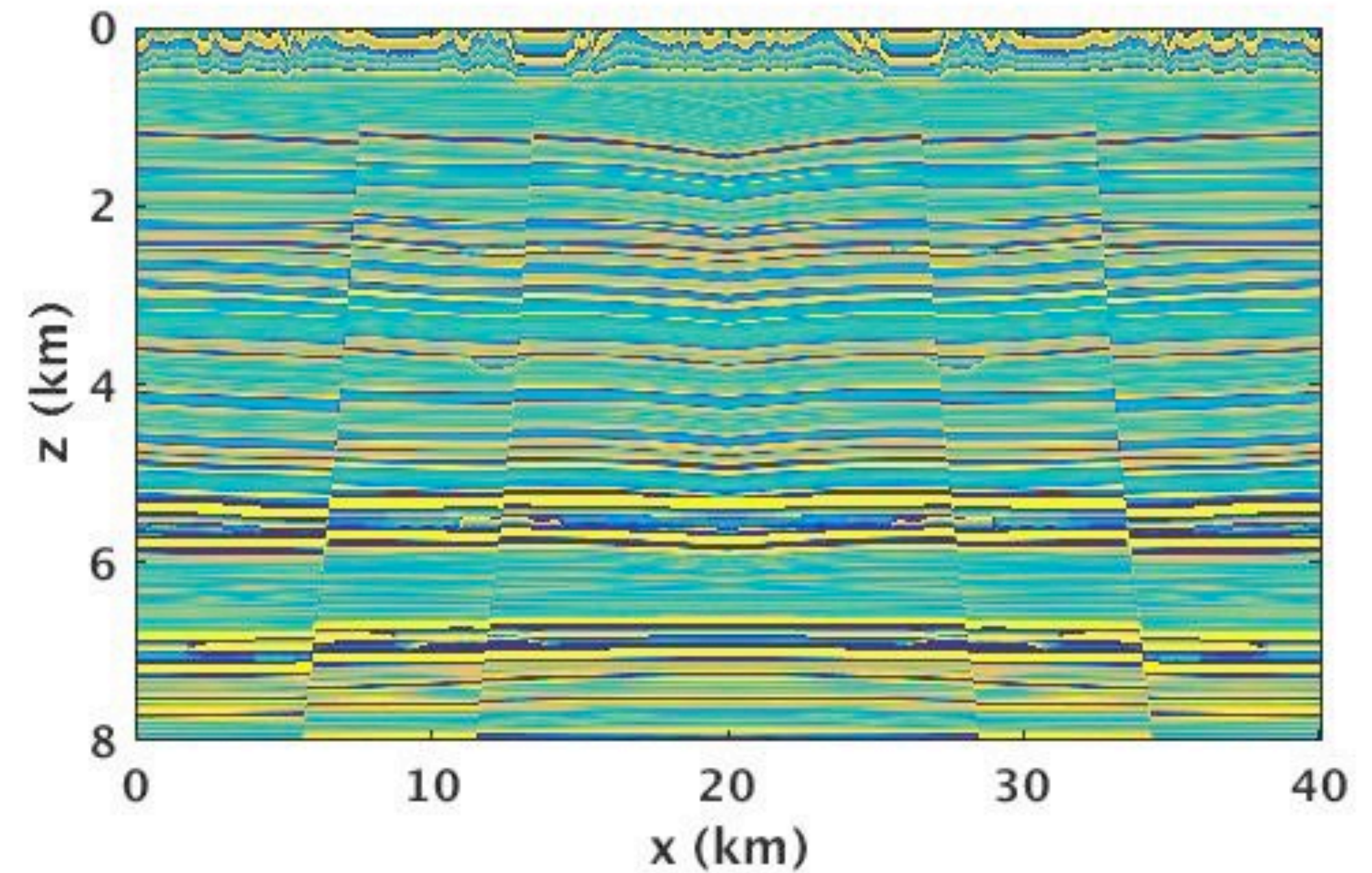
2D SEAM Model

SEAM Land Model

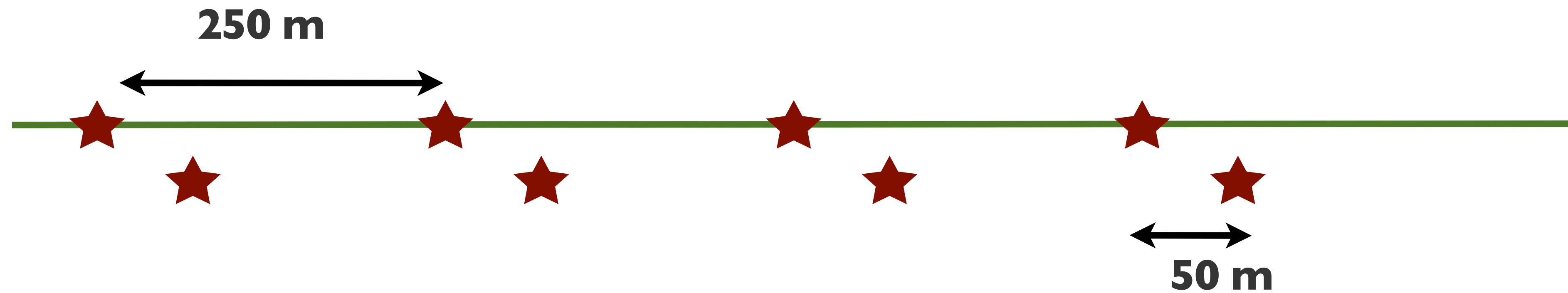
True



Perturbation



Acquisition parameters



720 sources and receivers sampled at 50 m

Four vibrators separated by 250 m

Green's function is simulated using ricker wavelet with central frequency of 25 Hz

Convolved w/ sweep to generate synthetic data

Acquisition parameters

Underlying grid:

720 sources and receivers sampled at 50 m

Four vibrators separated by 250 m

Ricker wavelet with central frequency of 25 Hz

4 – 5 X cost reduction

- thanks to CS based acquisition design

Optimization information

Parallelized factorization framework over sources & receivers

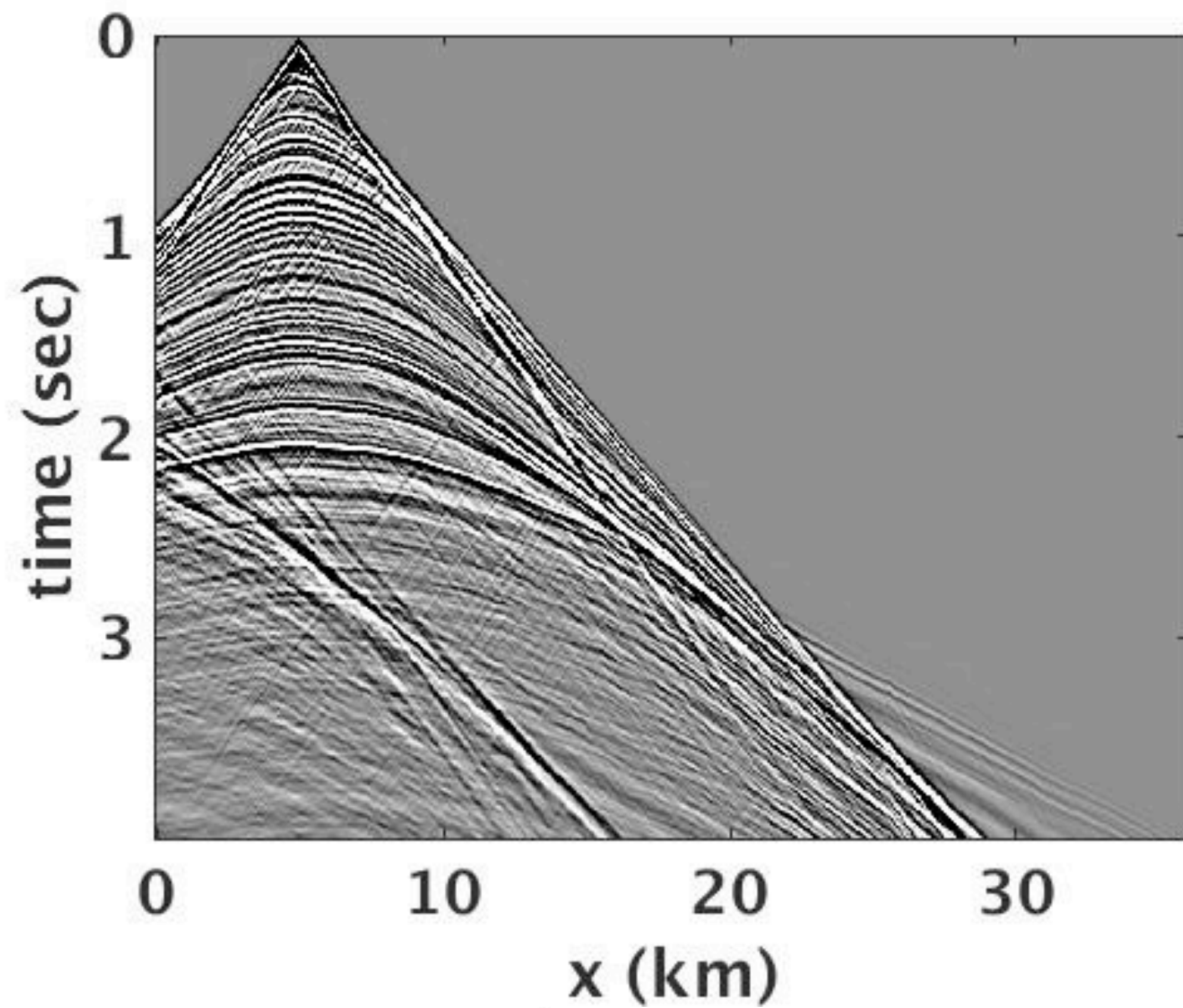
Number of iterations: 200

Computational time / frequency slice: 1 hour 10 minutes

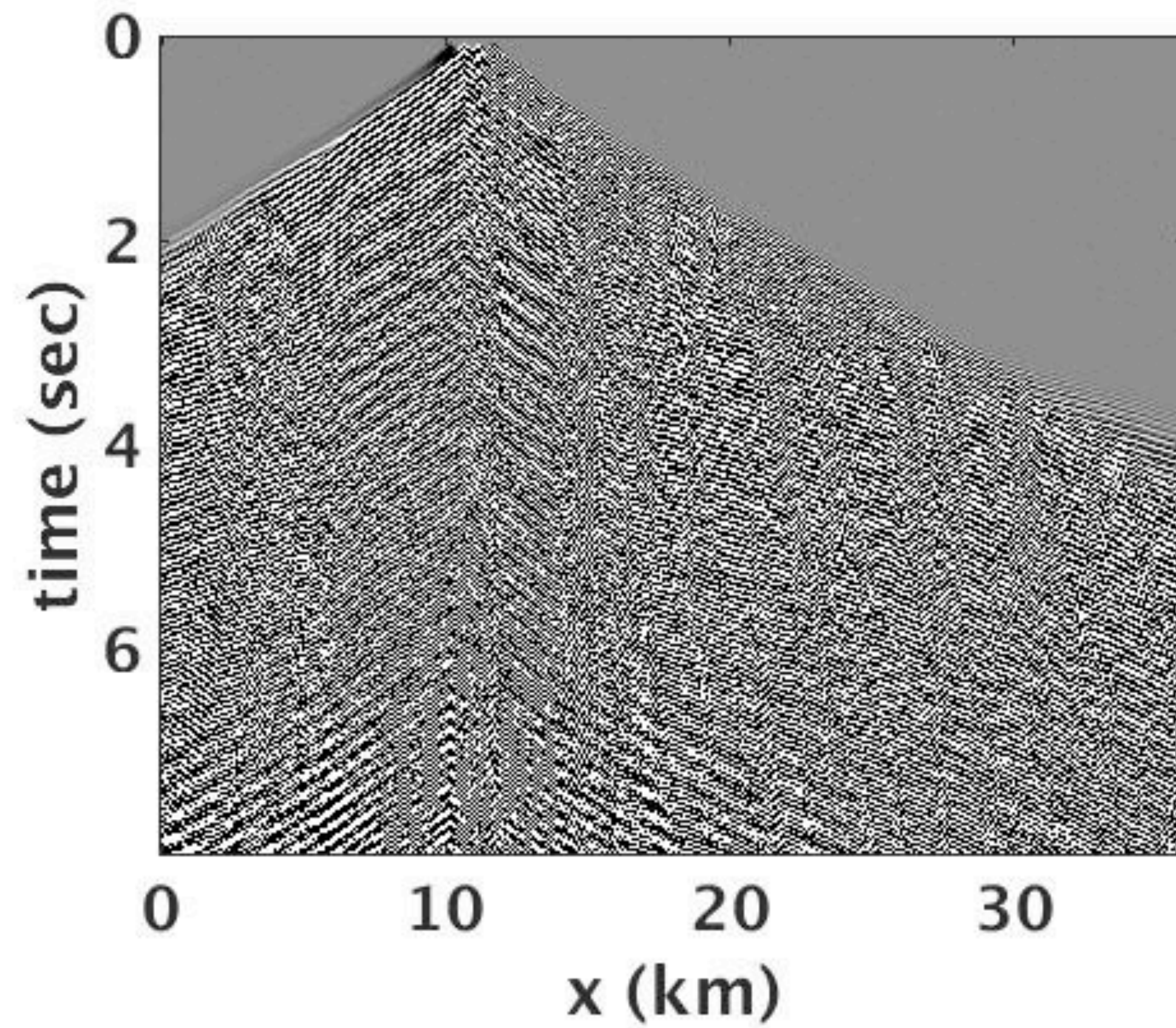
Computational resource / frequency slice: 1 node w/ 128 GB RAM, 20-core processors, and multithreading

Deblending and Spectral Interpolation

True

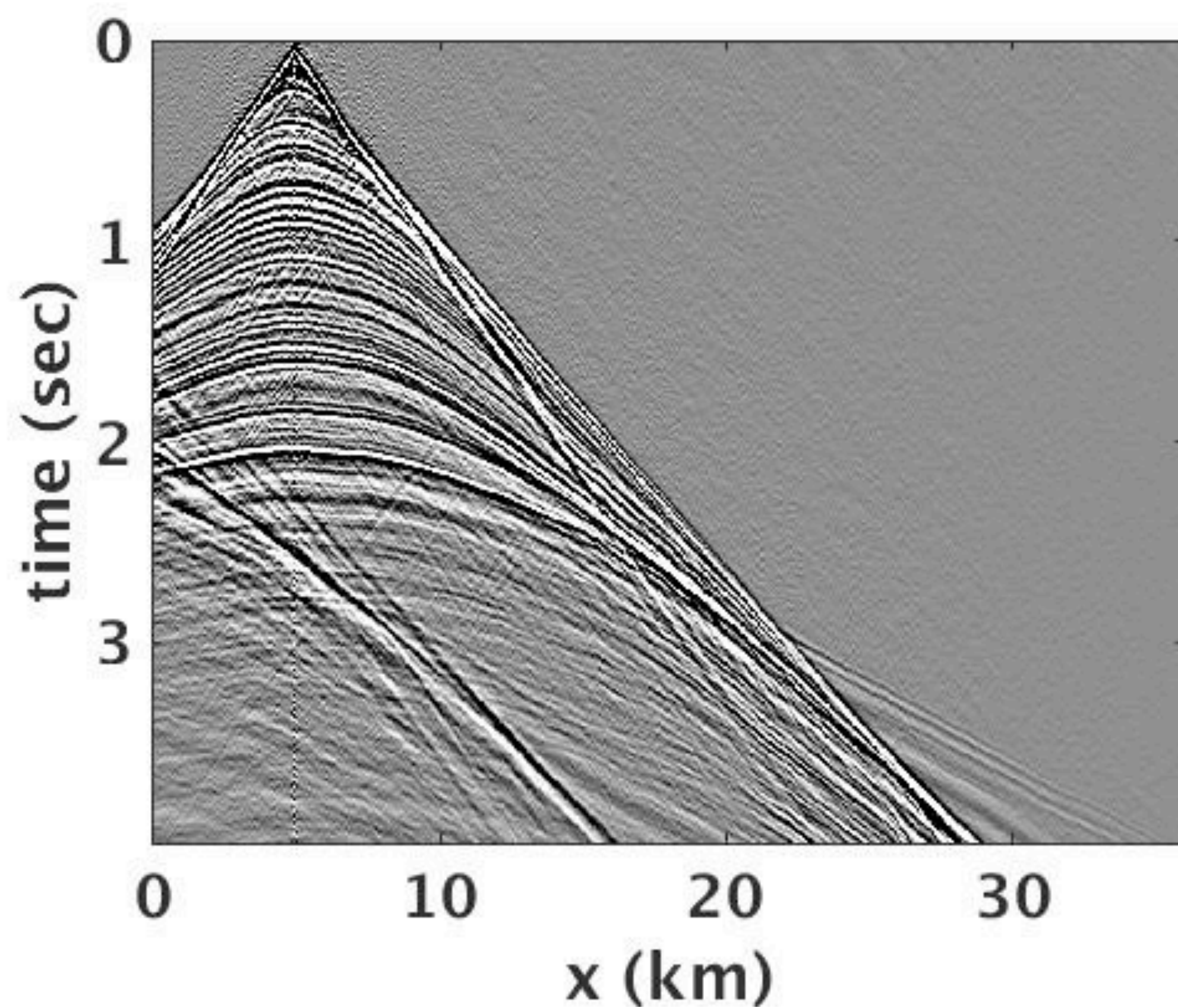


Blended data

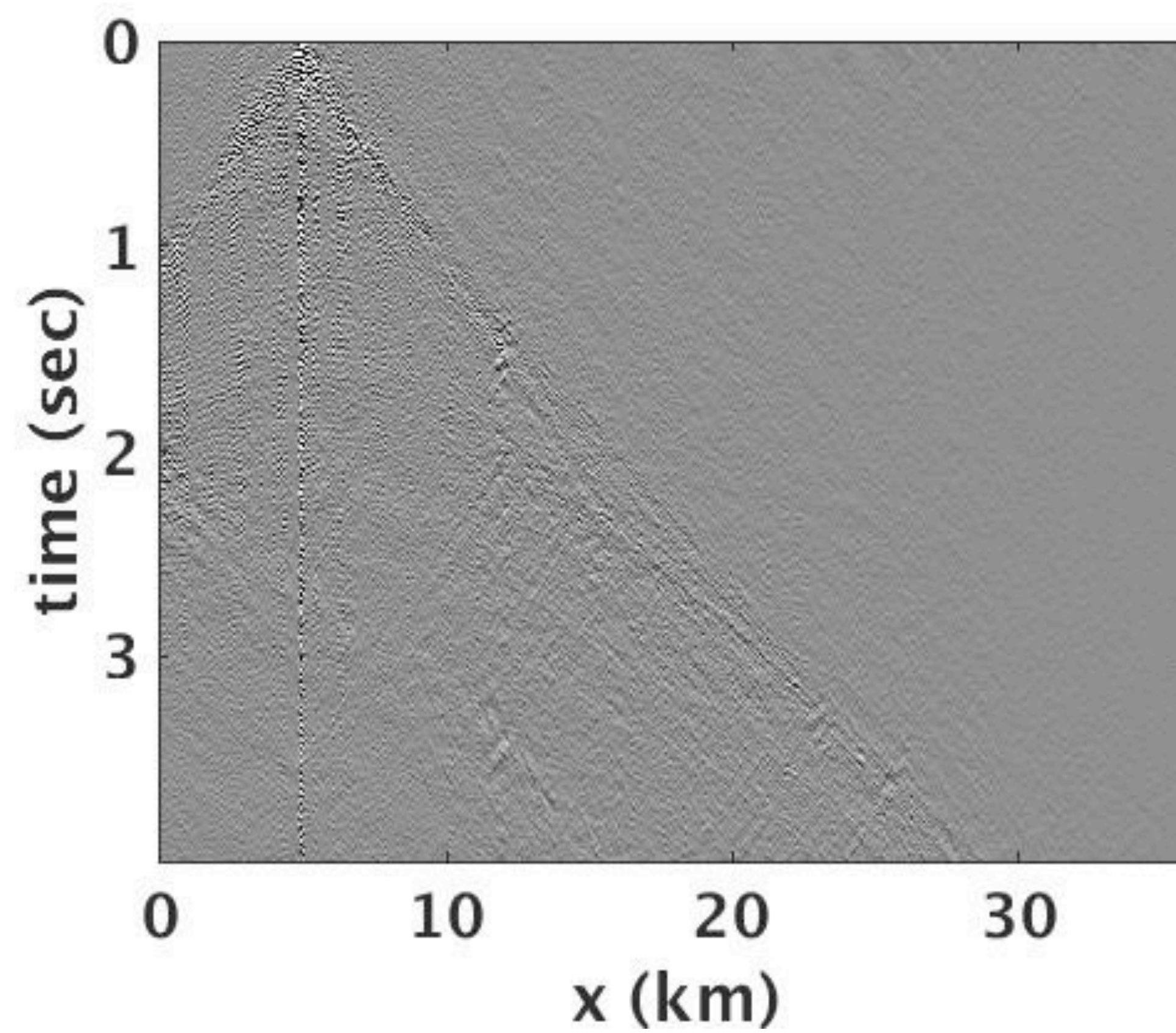


Deblending and Interpolation

Recovery
SNR = 21 dB

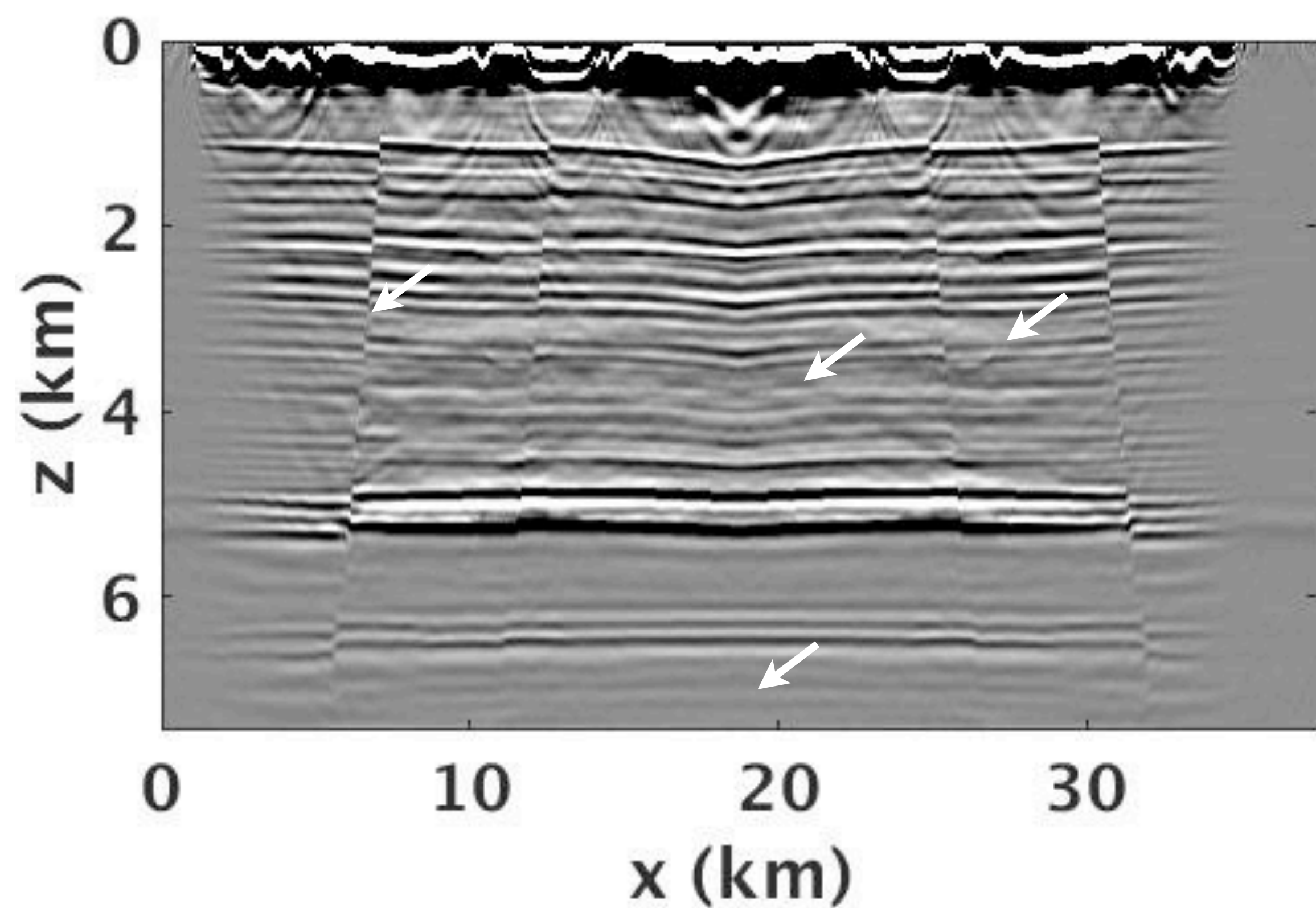


Residual

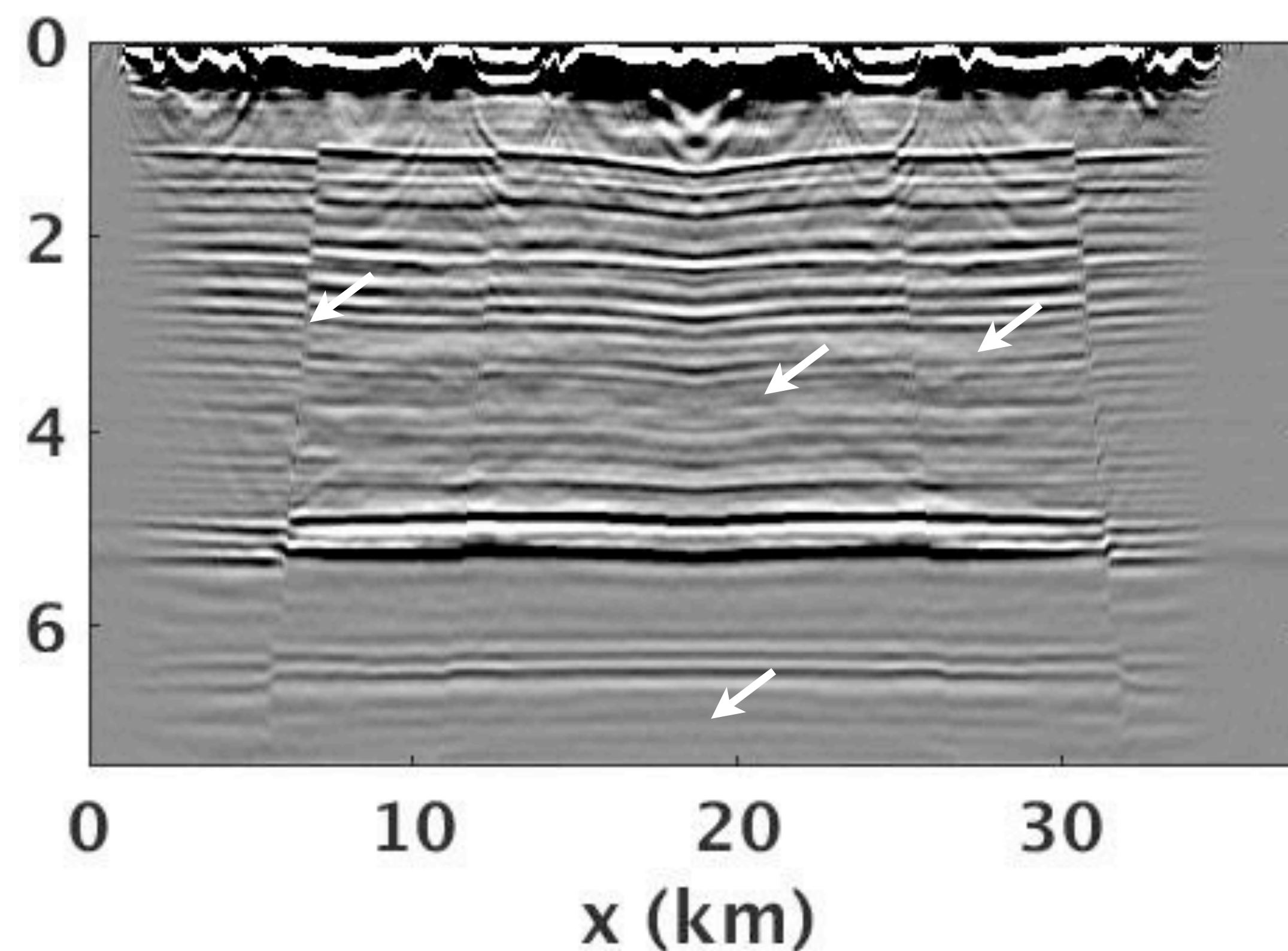


Reverse time migration

True

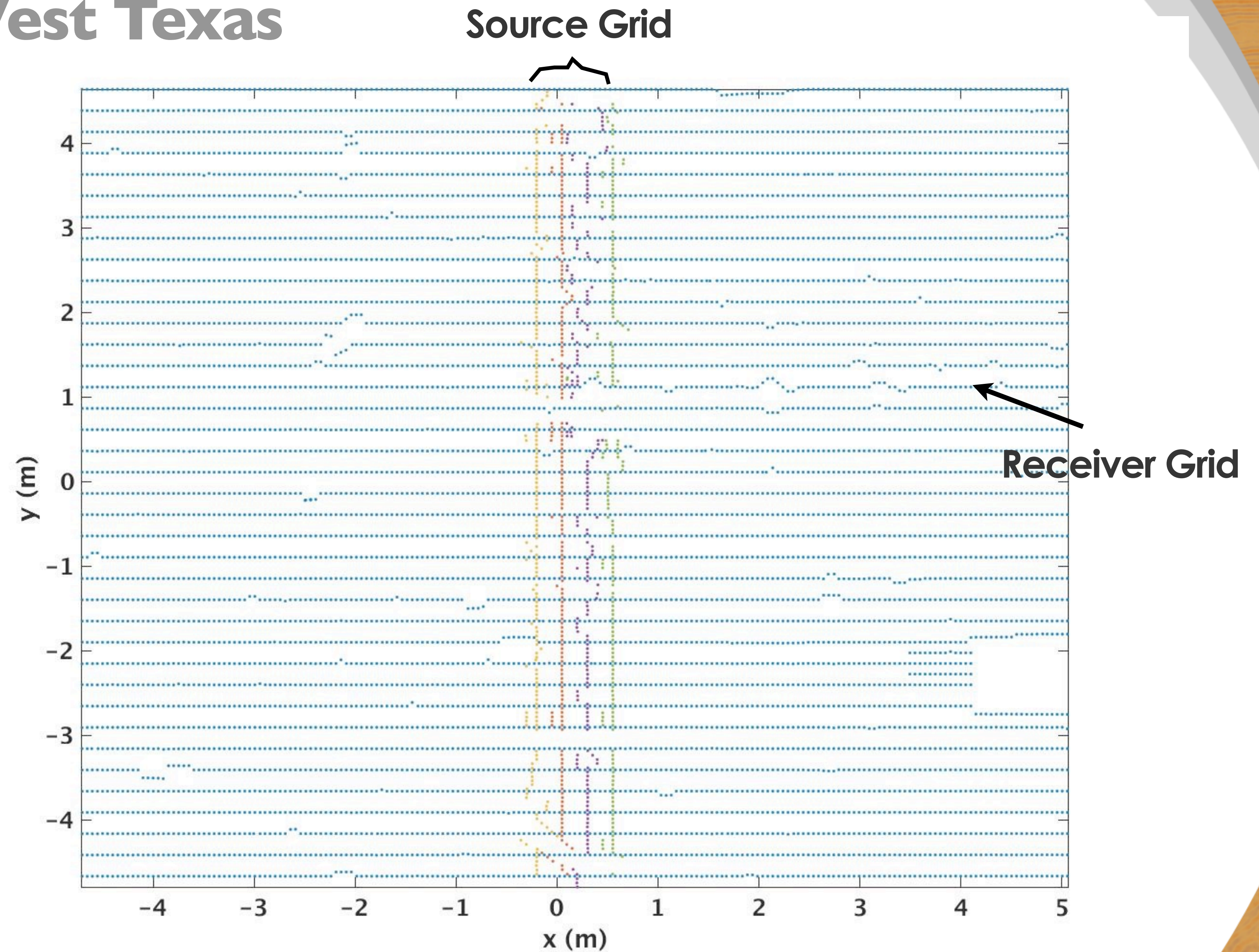


After deblending & Spectral Interpolation



3D Acquisition — West Texas

Real data—West Texas



Acquisition Parameters

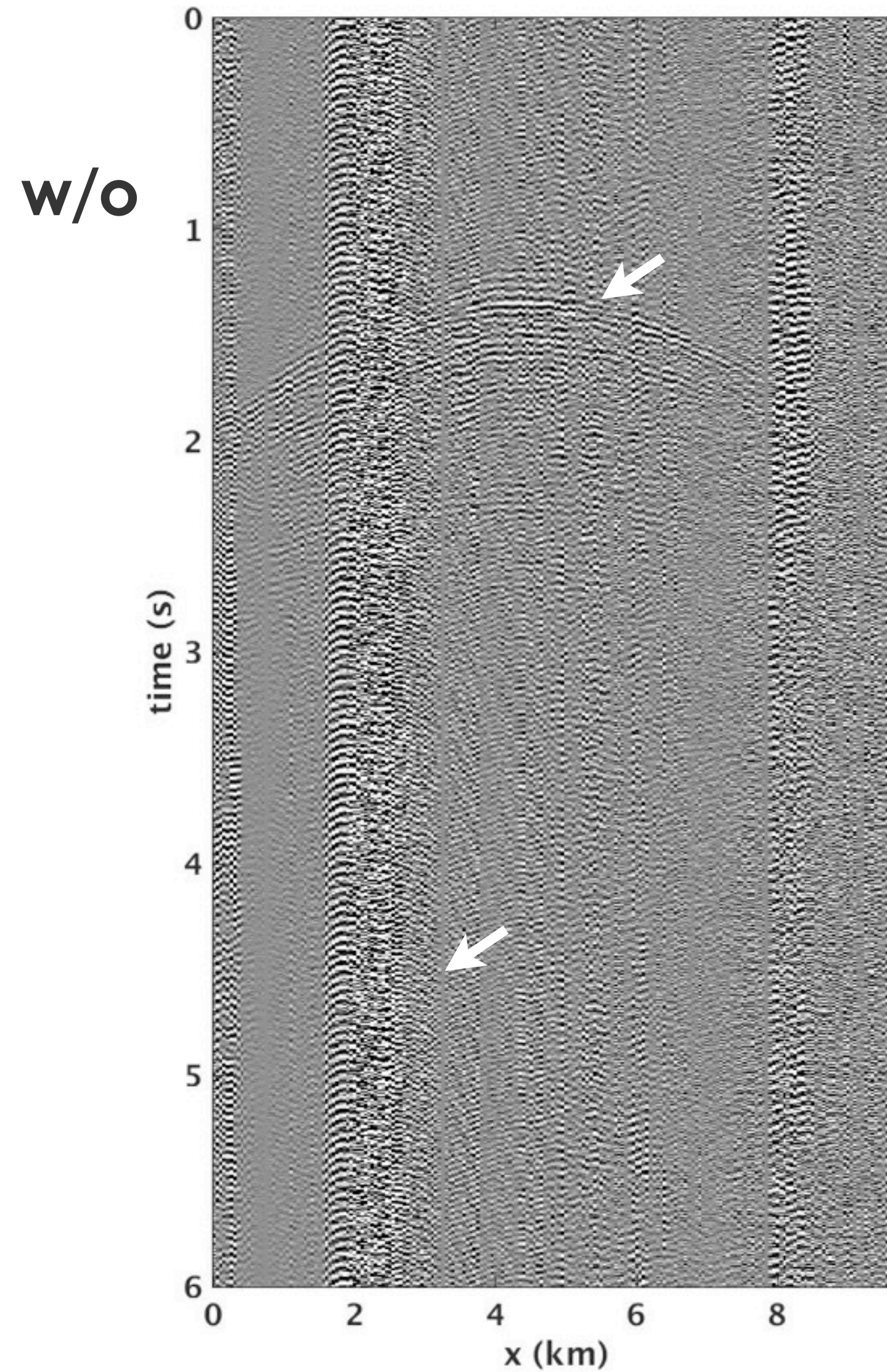
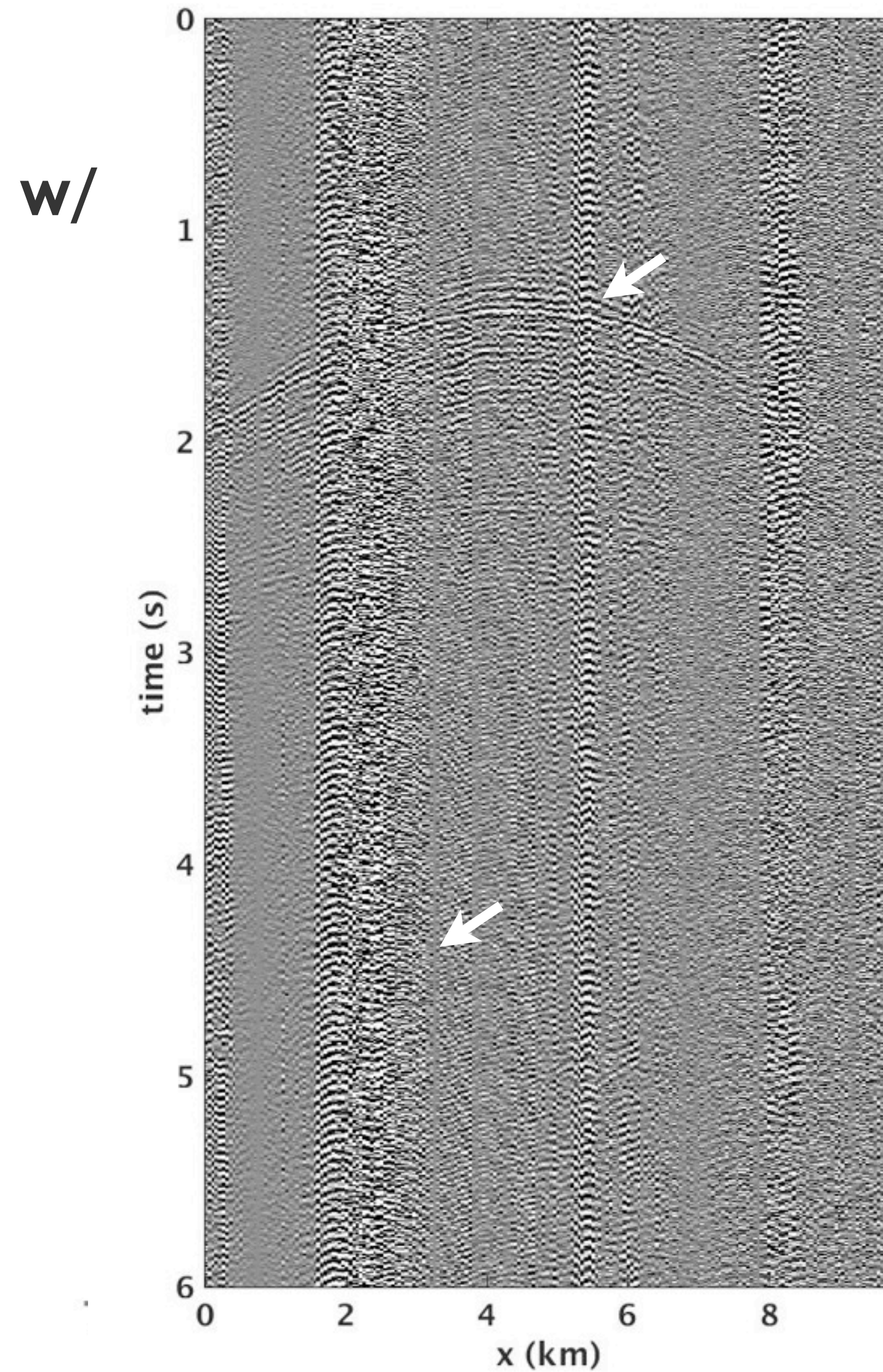
Source line interval = Receiver line interval = 825 ft

Source point interval=receiver point interval=165 ft

756 shots, 7400 receiver for each shot

4 different sweeps combination

Adjoint w/ & w/o sweeps subsampling



Benefits

4-5x speedup in acquisition

record less noise

Deblending and Spectral Interpolation process

Apply adjoint

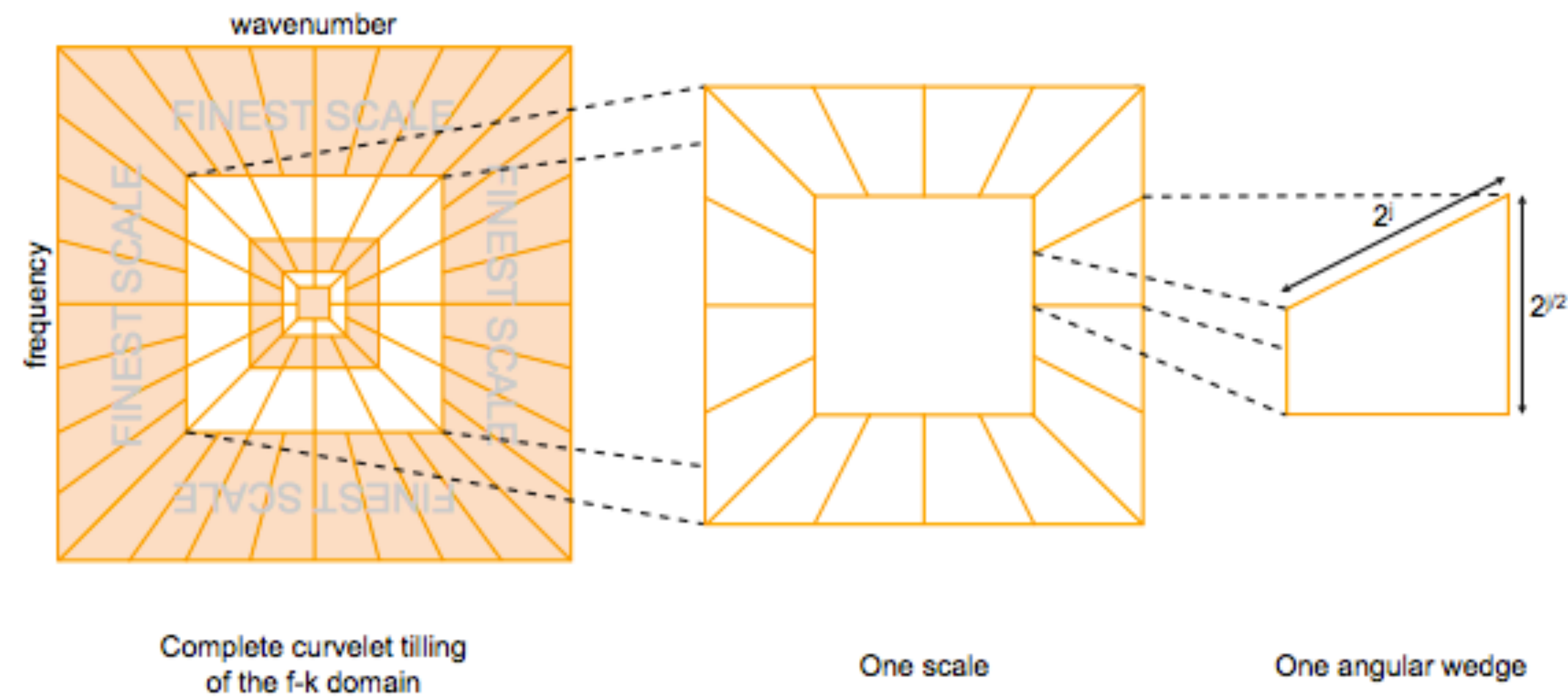
Remove ground roll

Blend ground roll and subtract from field data

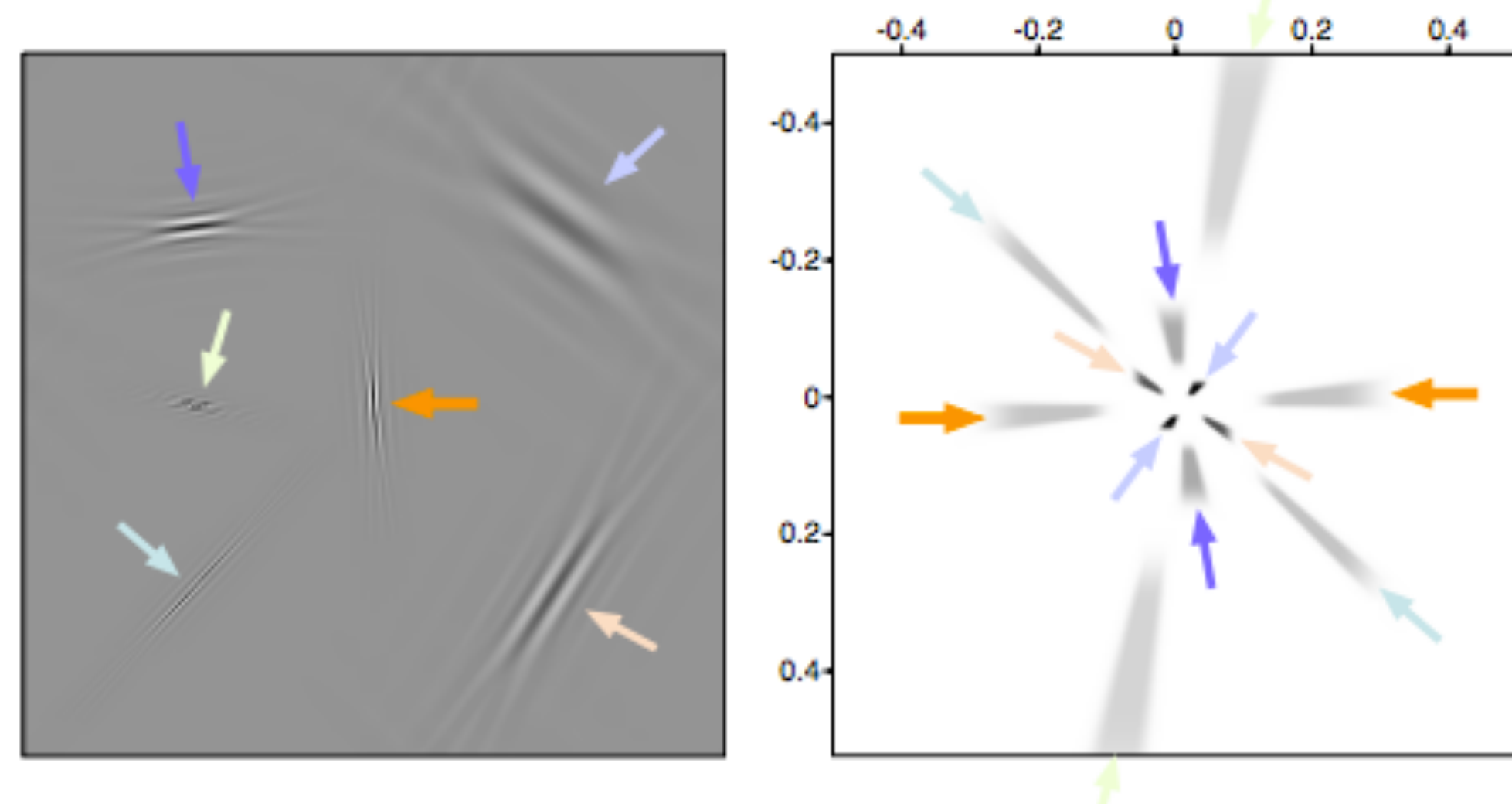
Run deblending & spectral interpolation

Ground roll removal

Curvelet transform



Curvelet mapping in FK domain



Noise mapping in curvelet domain

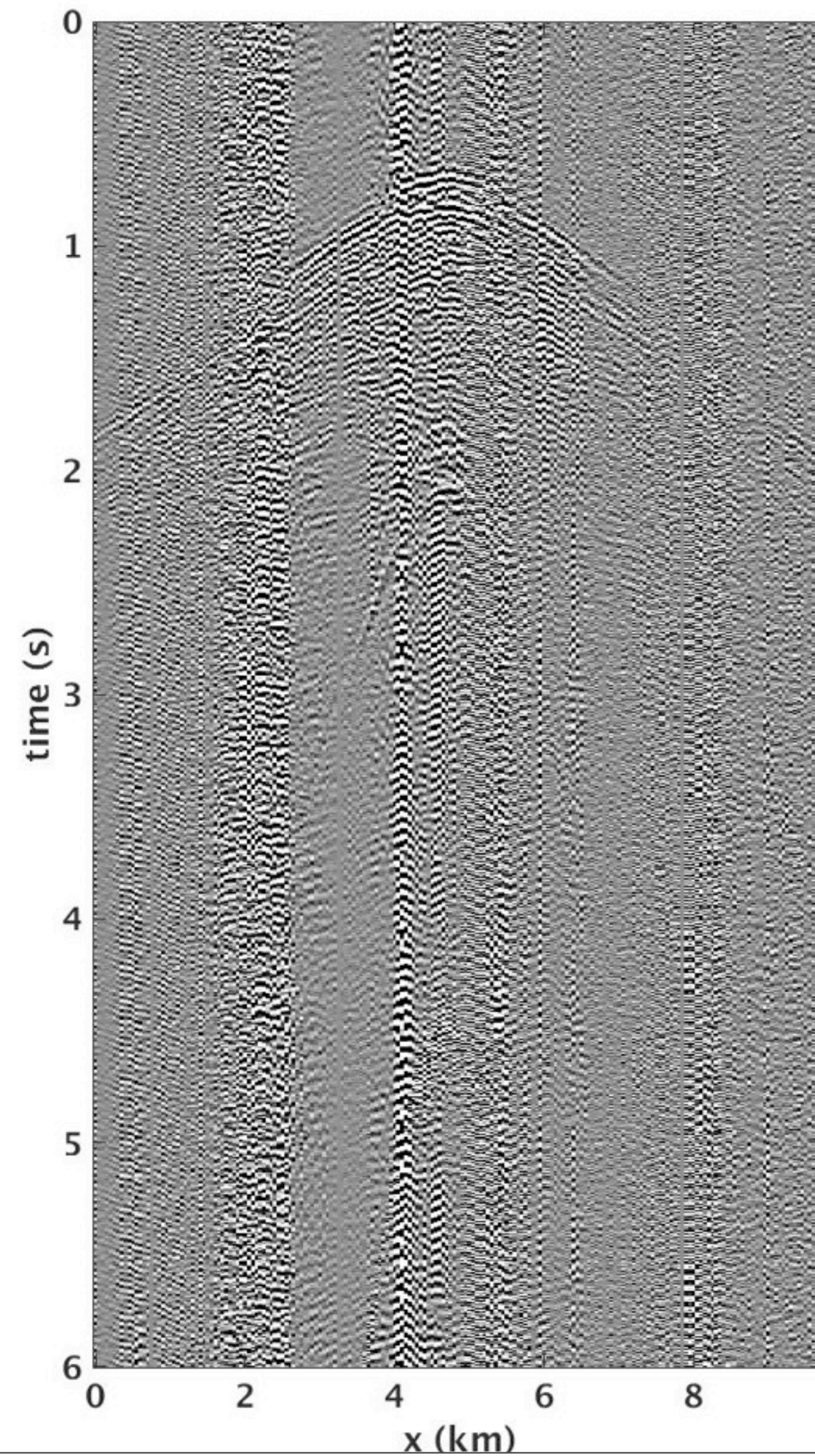
Different morphological appearances of noise & signal in curvelet domain

Noise & signal map to different angular wedges w/ distinct dip characteristics

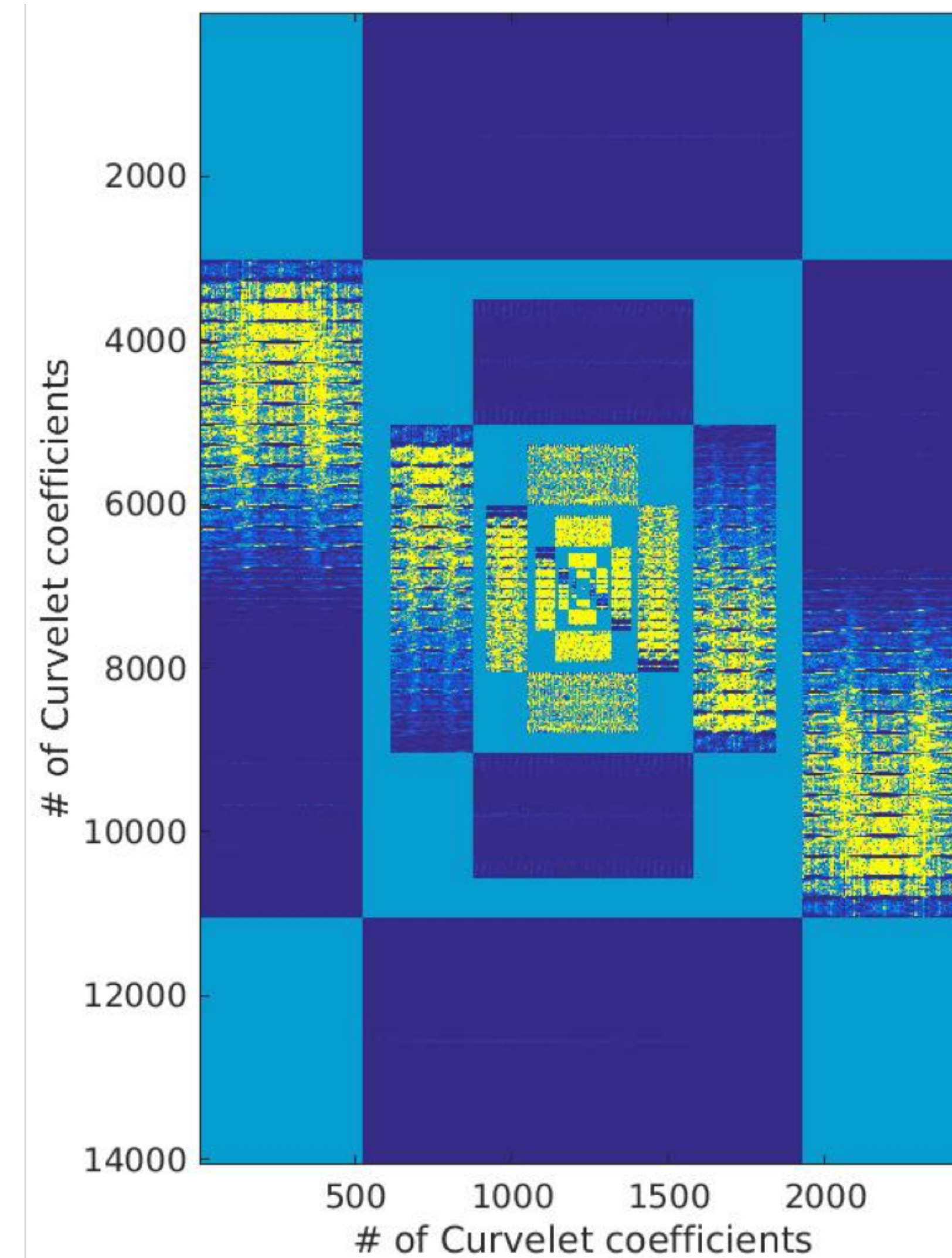
Coherent noise is generally low-rank

Seismic reflection & diving waves are sparse

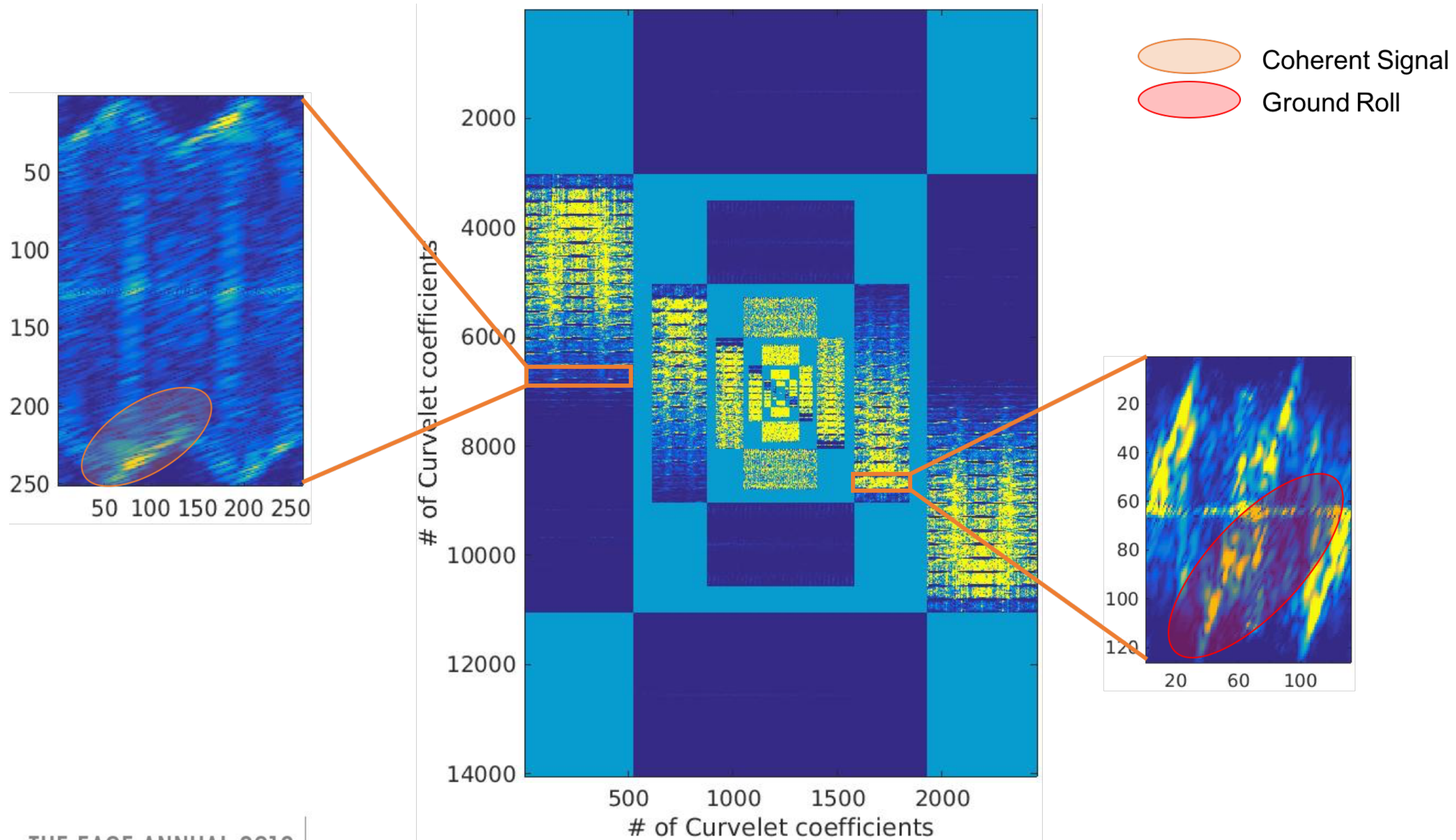
Curvelet representation



**Forward Curvelet
transform**



Ground roll in curvelet domain



Principal component pursuit

Let $\mathbf{Y} = \mathbf{L} + \mathbf{S}$, where \mathbf{Y} is observed data, \mathbf{L} is low-rank noise component and \mathbf{S} is sparse seismic reflection and diffraction events.

Principle component pursuit solves:

$$\min_{(\mathbf{L}, \mathbf{S})} \quad \|\mathbf{L}\|_* + \lambda \|\mathbf{S}\|_1 \quad \text{subject to} \quad \mathbf{L} + \mathbf{S} = \mathbf{Y},$$

where

$$\|\mathbf{L}\|_* = \sum_i \sigma_i(\mathbf{L}) \quad \text{and} \quad \|\mathbf{S}\|_1 = \sum_{i,j} |\mathbf{S}_{i,j}|$$

Principal component pursuit

Solve the following augmented Lagrangian system:

$$l(\mathbf{L}, \mathbf{S}, \mathbf{P}) = \min_{(\mathbf{L}, \mathbf{S}, \mathbf{P})} \quad \|\mathbf{L}\|_* + \lambda \|\mathbf{S}\|_1 + \langle \mathbf{P}, \mathbf{Y} - \mathbf{L} - \mathbf{S} \rangle + \frac{\mu}{2} \|\mathbf{Y} - \mathbf{L} - \mathbf{S}\|_F^2$$

Use alternating direction method

Each variable is solved using gradient decent followed by soft-thresholding

Principal component pursuit

Initialize $\mathbf{S}_0 = \mathbf{P}_0 = \mathbf{0}, \mu > 0, \lambda > 0$

for $k = 0, \dots, n$

$$\mathbf{L}_{k+1} = \mathcal{D}_{\mu^{-1}}(\mathbf{Y} - \mathbf{S}_k + \mu^{-1}\mathbf{P}_k)$$

$$\mathbf{S}_{k+1} = \mathcal{S}_{\lambda\mu^{-1}}(\mathbf{Y} - \mathbf{L}_{k+1} + \mu^{-1}\mathbf{P}_k)$$

$$\mathbf{P}_{k+1} = \mathbf{P}_k + \mu(\mathbf{Y} - \mathbf{L}_{k+1} - \mathbf{S}_{k+1})$$

end

where

$$\mathcal{S}_{\tau}[x] = \text{sgn}(x) \times \max(\|x\| - \tau, 0)$$

$$\mathcal{D}_{\tau}[\mathbf{X}] = \mathbf{U}\mathcal{S}_{\tau}(\mathbf{\Sigma})\mathbf{V}^*$$

Denoising framework

Perform 2D curvelet transform on each shot gather

Extract noisy curvelet coefficients along parabolic angular wedges at each scale and organize into a matrix

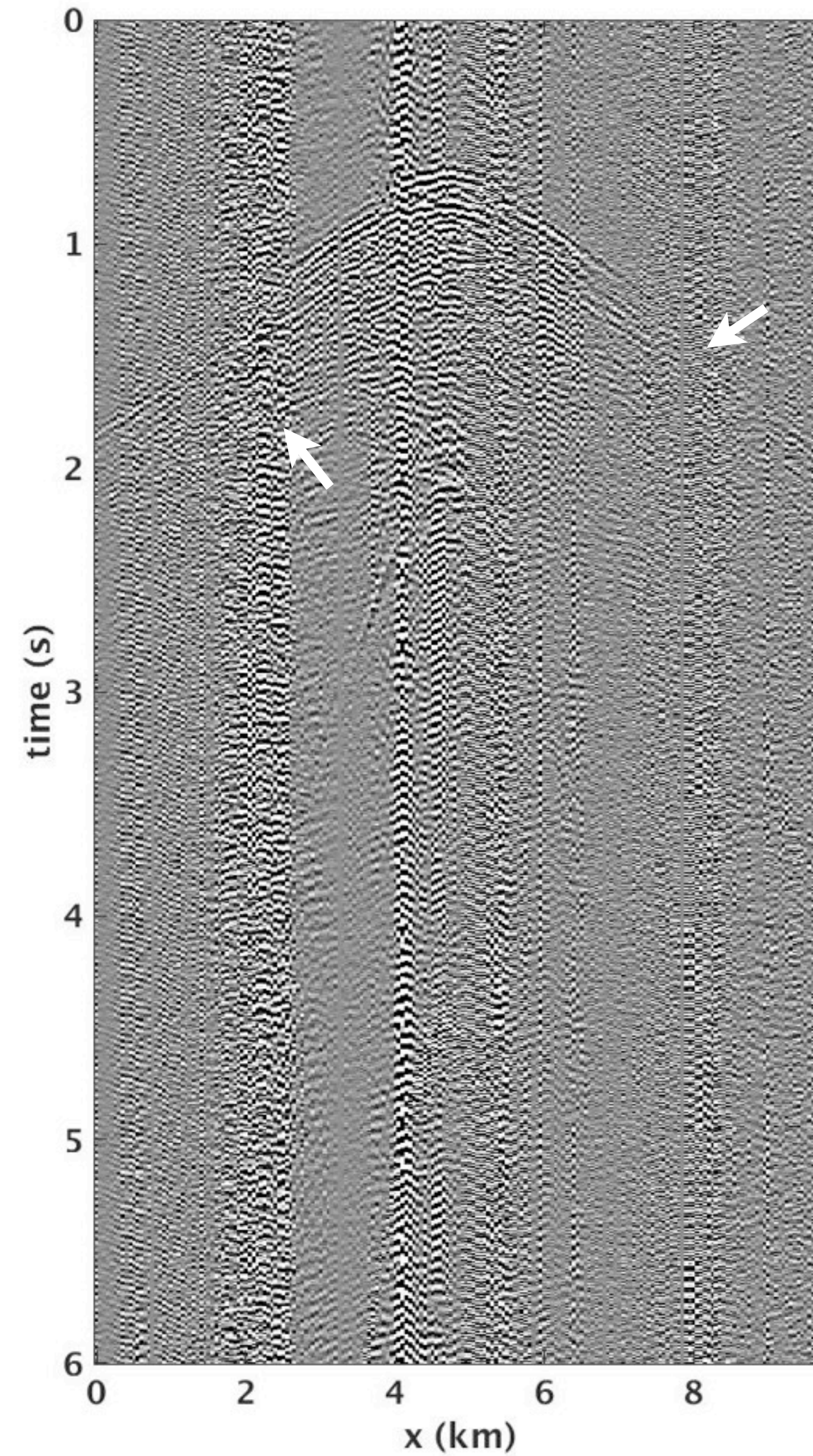
Solve RPCA on each of these matrices independently to separate the low-rank noise from the sparse component

Insert the separated curvelet coefficients for each scale back into the corresponding parabolic angular wedges

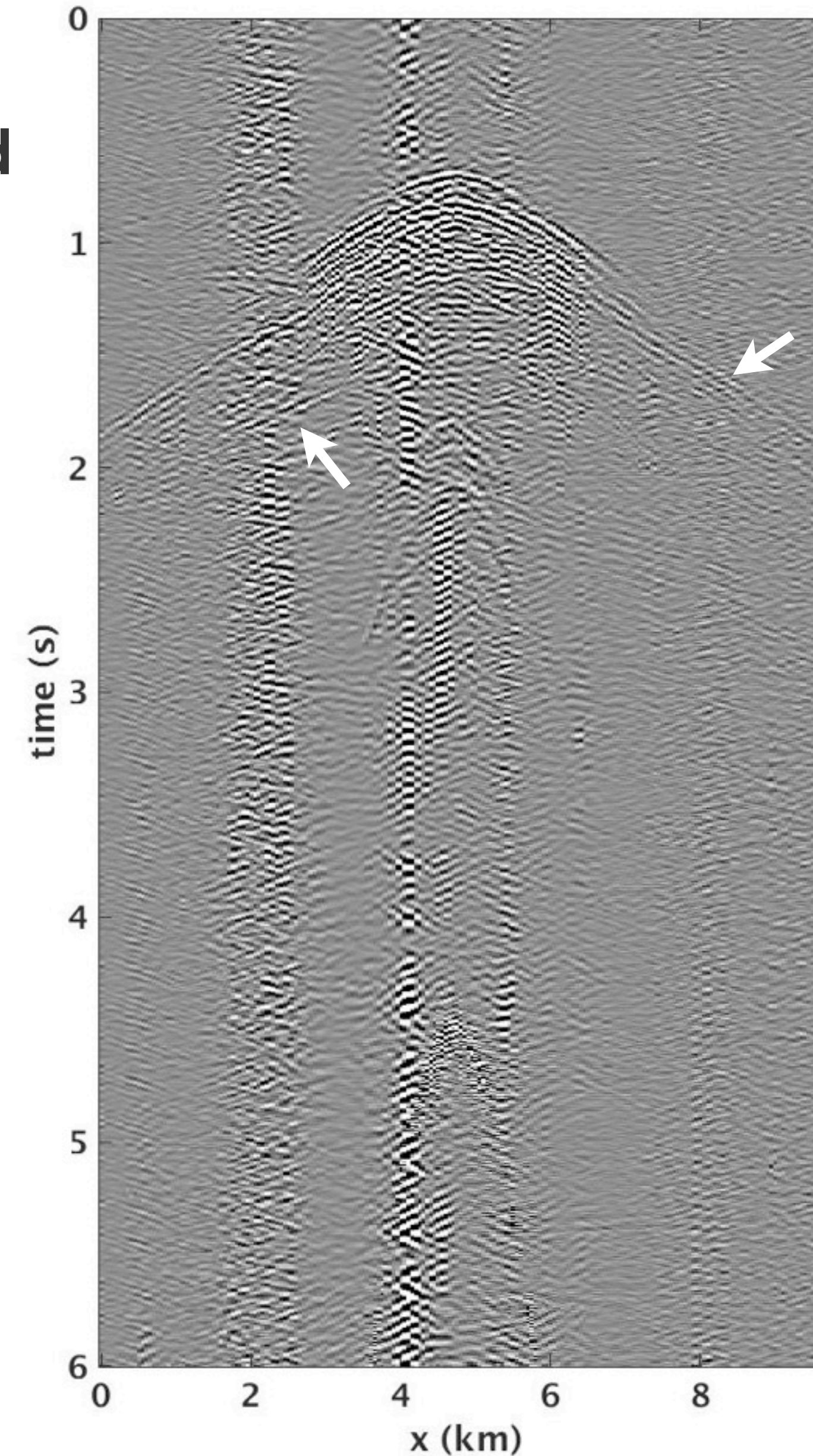
Perform 2D inverse curvelet transform to get estimates for shot records for the separated components

Curvelet based PCP

True

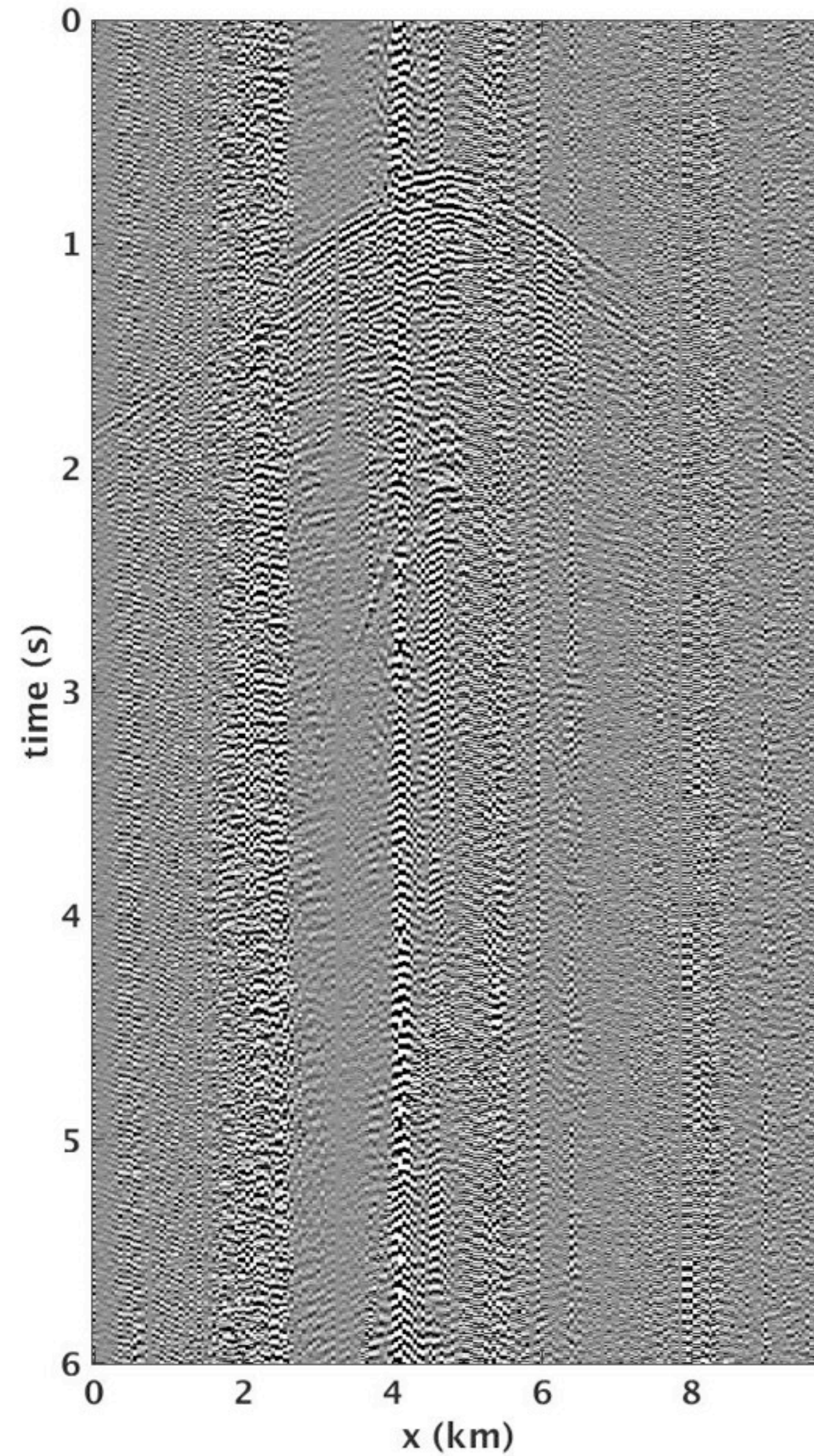


Denoised

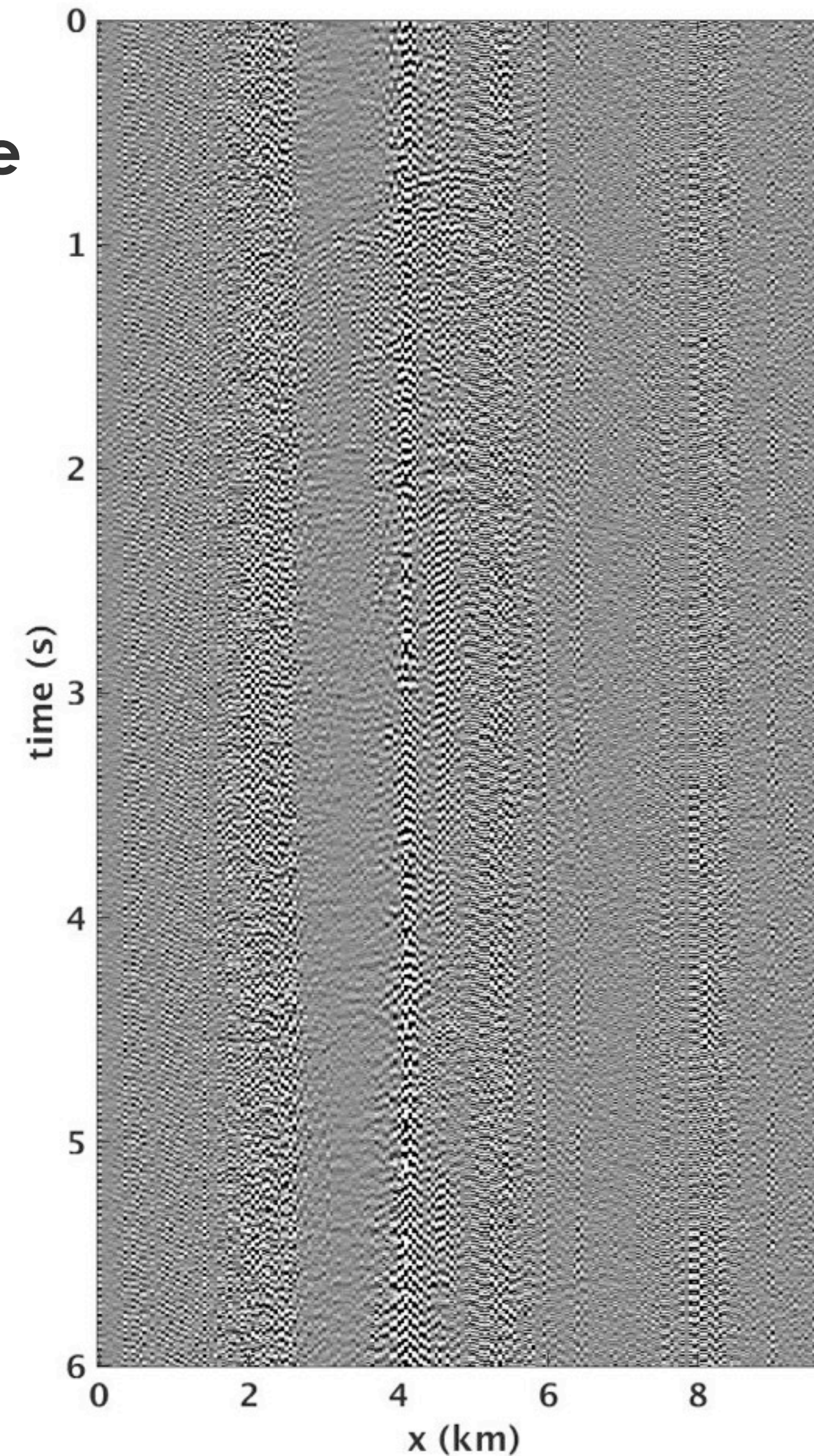


Curvelet based PCP

True



Difference



Future directions

Perform noise attenuation on field data before cross-correlation

Use robust-norm to minimize residual noise during inversion process

Re-design acquisition with more randomness across sources and receivers positions

Test random sweep encoding

Acknowledgements

This research was carried out as part of the SINBAD project with the support of the member organizations of the SINBAD Consortium.





EAGE ANNUAL
80TH CONFERENCE + EXHIBITION
COPENHAGEN | DENMARK

Thank you for your attention